



## RESEARCH ARTICLE

10.1029/2023GC011305

# Metamorphic Inheritance, Lower-Crustal Earthquakes, and Continental Rifting

Å. Fagereng<sup>1,2</sup> , J. F. A. Diener<sup>2</sup> , C. J. Tulley<sup>1,3</sup> , and B. Manda<sup>4</sup> 

<sup>1</sup>School of Earth and Environmental Sciences, Cardiff University, Cardiff, UK, <sup>2</sup>Department of Geological Sciences, University of Cape Town, Rondebosch, South Africa, <sup>3</sup>Now at RSC Mining & Mineral Exploration, Dunedin, New Zealand, <sup>4</sup>Chancellor's College, University of Malawi, Zomba, Malawi

### Key Points:

- The Malawi crust is mostly dry, metastable and frictionally strong, and rifting requires viscous flow in inherited lower crustal shear zones
- Major faults are likely to grow from below, with their location and orientation prescribed by underlying inherited viscous shear zones
- Viscous flow in heterogeneous crust may trigger lower crustal seismicity generating permeability that allows infiltration of external fluids

### Correspondence to:

Å. Fagereng,  
fagerenga@cardiff.ac.uk

### Citation:

Fagereng, Å., Diener, J. F. A., Tulley, C. J., & Manda, B. (2024). Metamorphic inheritance, lower-crustal earthquakes, and continental rifting. *Geochemistry, Geophysics, Geosystems*, 25, e2023GC011305. <https://doi.org/10.1029/2023GC011305>

Received 17 OCT 2023

Accepted 18 FEB 2024

### Author Contributions:

**Conceptualization:** Å. Fagereng, J. F. A. Diener, B. Manda

**Formal analysis:** Å. Fagereng, J. F. A. Diener, C. J. Tulley

**Funding acquisition:** Å. Fagereng

**Investigation:** Å. Fagereng, J. F. A. Diener, C. J. Tulley

**Methodology:** Å. Fagereng, J. F. A. Diener, B. Manda

**Project administration:** Å. Fagereng

**Supervision:** Å. Fagereng, J. F. A. Diener

**Validation:** B. Manda

**Visualization:** Å. Fagereng, J. F. A. Diener, C. J. Tulley

**Writing – original draft:** Å. Fagereng, C. J. Tulley

**Writing – review & editing:** J. F. A. Diener, B. Manda

**Writing – review & editing:** J. F. A. Diener, B. Manda

**Writing – review & editing:** J. F. A. Diener, B. Manda

**Writing – review & editing:** J. F. A. Diener, B. Manda

**Writing – review & editing:** J. F. A. Diener, B. Manda

**Writing – review & editing:** J. F. A. Diener, B. Manda

**Abstract** The Malawi Rift is localized within Precambrian amphibolite-granulite facies metamorphic belts, bounded by up to 150 km long border faults, and generates earthquakes throughout ~40 km thick crust. Rift-related faults are inferred to exploit pre-existing weaknesses that allow rifting of otherwise dry and strong crust. It is unclear what these weaknesses are, and how localization into weak zones can be reconciled with strength required for lower crustal seismicity. We present results of mineral equilibria modeling, which indicate that Proterozoic metamorphism generated dry crust dominated by a quartz-feldspar assemblage that is metastable at current conditions. For rift propagation to be possible at current cool thermal gradients and in mechanically strong, dry quartzofeldspathic rocks, mid- to lower-crustal strain must be localized into relatively weak, inherited shear zones that deform primarily by aseismic, viscous creep. These shear zones are embedded within high-strength crust, and interaction between creeping shear zones and enveloped or surrounding rocks may locally increase stress and trigger frictional, seismic slip at mid- to lower-crustal depths. Over time, this interaction may produce a fracture network that allows infiltration of fluids. We therefore suggest that during rifting of previously deformed and metamorphosed crust, major faults are most likely to grow from below, with their location and orientation prescribed by underlying inherited viscous shear zones. In this case, fluids may infiltrate and locally weaken metastable lower crust, including allowing time-dependent fluid-driven seismicity and local partial melting, but length-scales of this weakening is limited by the scale of the permeability network.

**Plain Language Summary** In Malawi, East Africa, the Earth's crust is slowly splitting apart. This “rifting” has two unusual characteristics: (a) the crust is thick and strong and therefore difficult to split apart, and (b) there are earthquakes at greater depth and temperature than typical for the continents. We propose that the reason rifting occurs with these two characteristics, in this location, is that the crust is inherited from past periods of mountain building. Based on thermodynamic principles, specifically what minerals are stable under what conditions, we model the composition of Malawi crust in the geological past. We then compare those results to current conditions. We find that the likely inherited composition of Malawi crust is unstable under current conditions, but needs an addition of water to undergo reactions to new, stable minerals. We also note that deformation is only possible in weak zones inherited from past deformation, and these zones will deform by high-temperature flow of rock, not generating earthquakes. However, flow of local weak zones may induce fracturing in surrounding harder rocks, generating local earthquakes and a fracture system that water can flow along. Over time, this water infiltration can weaken the crust and ultimately allow continental rifting as seen further north in Africa.

## 1. Introduction

Crustal-scale tectonic processes—including the continental rifting and mountain building events that define a Wilson Cycle—require deformation of the lower crust. There are, however, conflicting models regarding the strength that resides in the lower crust relative to the upper crust and lithospheric mantle, and by what mechanism (s) the lower crust can deform (Brace & Kohlstedt, 1980; W. P. Chen & Molnar, 1983; Jackson et al., 2004; Maggi et al., 2000; McKenzie & Fairhead, 1997). Strength is not a constant in time; evolution and internal differentiation of continental crust occurs through metamorphic and magmatic processes such as dehydration and melting, and these processes exert short- and long-term influences on the strength of the lower crust. For example, dehydration of low-permeability rocks may lead to short-term embrittlement because increased pore fluid pressures decrease effective stress (e.g., Etheridge et al., 1984; Norris & Henley, 1976; Yardley, 1983, 1986), while ultimately increasing the long-term strength of the rocks by breaking down relatively weak hydrous minerals and removing

grain-boundary fluids (e.g., Tenczer et al., 2006; White & Powell, 2002). Similarly, melting first induces temporary weakening due to an increase in the volume and interconnectivity of low-viscosity melt (Rosenberg & Handy, 2005), but the mobility and subsequent removal of melt ultimately increases the long-term strength of the affected rocks by making them drier and volumetrically dominated by strong residual minerals (Brown, 1994; Diener & Fagereng, 2014; White & Powell, 2002). These changes are difficult to reverse, and the dry and residual mineralogy and resultant strength will commonly persist under subsequent retrograde conditions and through overprinting tectonic events (Austrheim & Boundy, 1994; Diener et al., 2008; Jackson et al., 2004; Jamtveit et al., 2019; Tenczer et al., 2006; White & Powell, 2002). Examples of such metamorphic inheritance are observed where older (generally Precambrian), previously deformed and metamorphosed crust experiences tectonic reactivation. In such cases, the relatively high crustal strength is reflected by earthquake depth-distributions throughout the continental crust (Maggi et al., 2000; Sloan et al., 2011).

In orogenic settings, local seismicity throughout the lower crust is inferred to be a consequence of local stress pulses within dry and strong rocks, creating permeability that then allows fluid-related weakening (Austrheim & Boundy, 1994; Jamtveit et al., 2018). This model requires a source of transient stress and connection to an external fluid source, which could involve earthquakes on overlying, permeable fault systems in a system driven “top-down” (Jamtveit et al., 2018). Under these conditions, the introduction of water into previously metamorphosed and dehydrated mid- to lower-crust may induce the growth of hydrous minerals such as phyllosilicates, reduce grain size, increase porosity and reaction kinetics, add a grain boundary fluid, and increase pore fluid pressure (Imber et al., 1997; Janecke & Evans, 1988; Stenvall et al., 2020; Wintsch et al., 1995; Yardley, 2009). This could lead to drastic but localized changes in rheology that, depending on the mineral-scale mechanism, may reduce strength and either induce local seismicity or lead to development of shear zones that accommodate viscous shear at low stress levels (Austrheim & Boundy, 1994; Fagereng & Diener, 2011; Jamtveit et al., 2019; Yardley, 2009). Transient earthquakes in inherited strong crust may therefore be agents of long-term weakening, but despite much interest, the processes that allow earthquakes to occur at lower-crustal pressures (that should be sufficiently high to suppress frictional sliding) and temperatures (that should be sufficiently high for efficient crystal-plastic creep) remain unclear.

The Malawi Rift is an example of actively rifting continental crust where present-day earthquakes occur from near-surface depths down to ~40 km (Camelbeeck & Iranga, 1996; Ebinger et al., 2019; Nyblade & Langston, 1995; Stevens et al., 2021). This maximum depth is consistent with estimates for the depth of the Moho (~40 ± 5 km; Borrego et al., 2018; Njinju et al., 2019a; Wang et al., 2019), indicating that the entire crust is seismogenic, and that there is no weak and aseismic mid- and lower crust present. Such a thick seismogenic zone is unusual for a region of active crustal extension, and it is also difficult to reconcile rifting of strong lower crust with the calculated available driving stresses (Buck, 2004; Kendall & Lithgow-Bertelloni, 2016; Stamps et al., 2014). The Malawi Rift is developing in ancient crust that has experienced multiple episodes of high-temperature metamorphism and deformation in the Proterozoic (De Waele & Mapani, 2002; Fritz et al., 2013; Manda et al., 2019; Ring et al., 1997), but has since experienced a period of relative tectonic quiescence (interrupted by episodes of intraplate magmatism and local Karoo and Cretaceous rifting) and cooling leading up to the current rifting episode. As such, the Malawi lower crust as a whole is likely to be dry and strong (Craig & Jackson, 2021; Fagereng, 2013; Jackson & Blenkinsop, 1993), yet initiation of rifting requires it to also have local weakness (Kendall & Lithgow-Bertelloni, 2016; Stamps et al., 2014).

Deep earthquakes observed elsewhere in the East African Rift system are thought to be related to lower-crustal fluid flow, involving mantle-derived magmas or fluids (e.g., Albaric et al., 2013; Ebinger et al., 2017; Gardonio et al., 2018; Lavayssi re et al., 2019; Lee et al., 2016; Roecker et al., 2017; Weinstein et al., 2017). Details of the type and source of fluids and their interaction with the lower-crustal rocks, however, remain speculative. As in orogens, earthquakes at the high confining stresses of the lower crust require a transient stress increase or local weakening, and neither process has been identified in the amagmatic rift setting. Here, we argue that metamorphic inheritance is key for localized lower-crustal seismicity, but such inheritance also limits the options for available weakening mechanisms. We use mineral equilibrium modeling to determine the likely mineralogy and fluid content of lower-crustal rocks prior to current rifting, based on the tectonic history of Malawi. With constraints from recently published heat flow calculations based on regional aeromagnetic data (Njinju et al., 2019b), we consider the stability of the inherited metamorphic assemblages at current conditions, and the effects of potential fluid addition during ongoing rifting. These calculations provide insights to the crustal conditions at which current

rifting began, and the potential interaction between ongoing rifting, metamorphic reactions, and lower-crustal seismicity.

## 2. Regional Geology, Tectonics, and Thermal Structure

### 2.1. Geological History

The Malawi Rift is part of the largely amagmatic Western Branch of the southern East African Rift, and extends for 900 km southwards from the Rungwe Volcanic Province in Tanzania to the Urema Graben in Mozambique (Ebinger et al., 1987). The Malawi Rift is characterized by a series of steeply dipping border-faults that have typical lengths of 75–150 km and segment the Rift into grabens and half-grabens (Figure 1) (Ebinger et al., 1987; Jackson & Blenkinsop, 1997; Laõ Dávila et al., 2015). The majority of the surface geology in the Rift region consists of Proterozoic granitic to granodioritic rocks that have been variably re-worked and metamorphosed during the Ubendian–Usagaran, Irumide, and Pan-African tectonic events (De Waele & Mapani, 2002; Fritz et al., 2013; Manda et al., 2019; Ring et al., 1997). Northern Malawi is underlain by Ubendian–Usagaran-aged metamorphic and magmatic rocks that experienced low- to high- $P$  granulite-facies metamorphic conditions (750–850°C at 0.5 GPa to ~880°C at 1 GPa) at  $c.$  2.0 Ga (Ring et al., 1997). Central and southern Malawi is underlain by rocks that likely experienced deformation and metamorphism related to both  $c.$  1.05 Ga Irumide and  $c.$  580–550 Ma Pan-African Mozambique Belt events (Fritz et al., 2013; Thomas et al., 2022; Tsunogae et al., 2021). In a regional reconstruction, Fritz et al. (2013) suggest that the crust west of Lake Malawi is dominated by Irumide rocks that acted as a relatively rigid indenter and only experienced minor to moderate reworking in the Pan-African. Conversely, the rocks east of Lake Malawi, namely the Unango Block in northern Mozambique/southern Malawi, are interpreted as Irumide rocks that experienced substantial tectonic and metamorphic reworking during Pan-African regional transpression (Figure 1). Both the Irumide and Pan-African tectonic events reached granulite facies conditions, with  $T$  in excess of 900°C at 0.5–0.6 GPa reported from the Irumide Belt in eastern Zambia (Karamakar & Schenk, 2016), and Pan-African conditions of 900°C at 1 GPa estimated for southern Malawi (Kröner et al., 2001).

Subsequent to the Pan-African transpression, continental-scale Karoo rifting that occurred primarily in the Permian-Triassic and culminated with the Jurassic Gondwana break-up led to the formation of several NE-SW trending sedimentary basins in Malawi (Figure 1; Castaing, 1991; Catuneanu et al., 2005). These sedimentary basins are confined to upper-crustal depths with Karoo sediments in Malawi reaching thicknesses of up to 3 km (Castaing, 1991; Geological Survey of Malawi, 1966), although this may be an under-estimate as significant thicknesses of Karoo sediments may have been eroded (McMillan et al., 2022). Although preserved in the topography and sedimentary record, faults defining the main NE-SW trending Karoo basins of Malawi show little sign of current tectonic reactivation (Figure 1a; Castaing, 1991). In northern Malawi, however, evidence is reported for N-striking Karoo-age faults, interpreted as an effect of them having reactivated Precambrian structures (Dawson et al., 2018), whereas some current major NW-striking rift features are interpreted to have been active as strike-slip faults during Karoo rifting (Castaing, 1991; Delvaux et al., 2012; Wedmore et al., 2020). Minor, local chlorite-epidote coatings with strike-slip lineations attest to some hydrothermal flow along these faults at Karoo times (Delvaux et al., 2012). Following the Karoo rifting, a minor phase of NE-SW directed extension is reported to have occurred in the Cretaceous (Castaing, 1991). This is associated with NW-striking fluvial sediments referred to as Dinosaur Beds, and reactivation of NW-SE striking crustal-scale faults including the Mughese Shear Zone (Castaing, 1991; Dawson et al., 2018). In addition to these faulting episodes, the Karoo was also associated with intrusion of NE-SW striking basaltic dykes, followed by alkaline intrusions of the Chilwa Alkaline Province (Carter & Bennet, 1973; Dixey et al., 1937). The Chilwa Province dates from the Jurassic to the Cretaceous, and contains ring complexes and dykes striking both NW-SE and NE-SW (Bloomfield, 1961; Geological Survey of Malawi, 1966). Castaing (1991) interpret these two dyke orientations as recording a rotation in the primary extension direction between Karoo and Cretaceous rifting in Malawi. The Chilwa Province, and several other intraplate African ring complexes, are proposed to have formed from a combination of asthenospheric and lower-crustal partial melting during extension localized to existing crustal-scale weaknesses (Nyulugwe et al., 2019; Vail, 1989). Some major faults are thought to have been reactivated repeatedly by post-Pan African deformation episodes, such as the Thyolo Fault (Wedmore et al., 2020) and the Mughese Shear Zone (Dawson et al., 2018); however, note that these are described as having minor near-surface alteration and remain dominated by high-grade metamorphic assemblages. Overall, the Karoo and Cretaceous deformation episodes involved reactivation of some crustal-scale shear zones and creation of some new, upper-crustal fault systems.

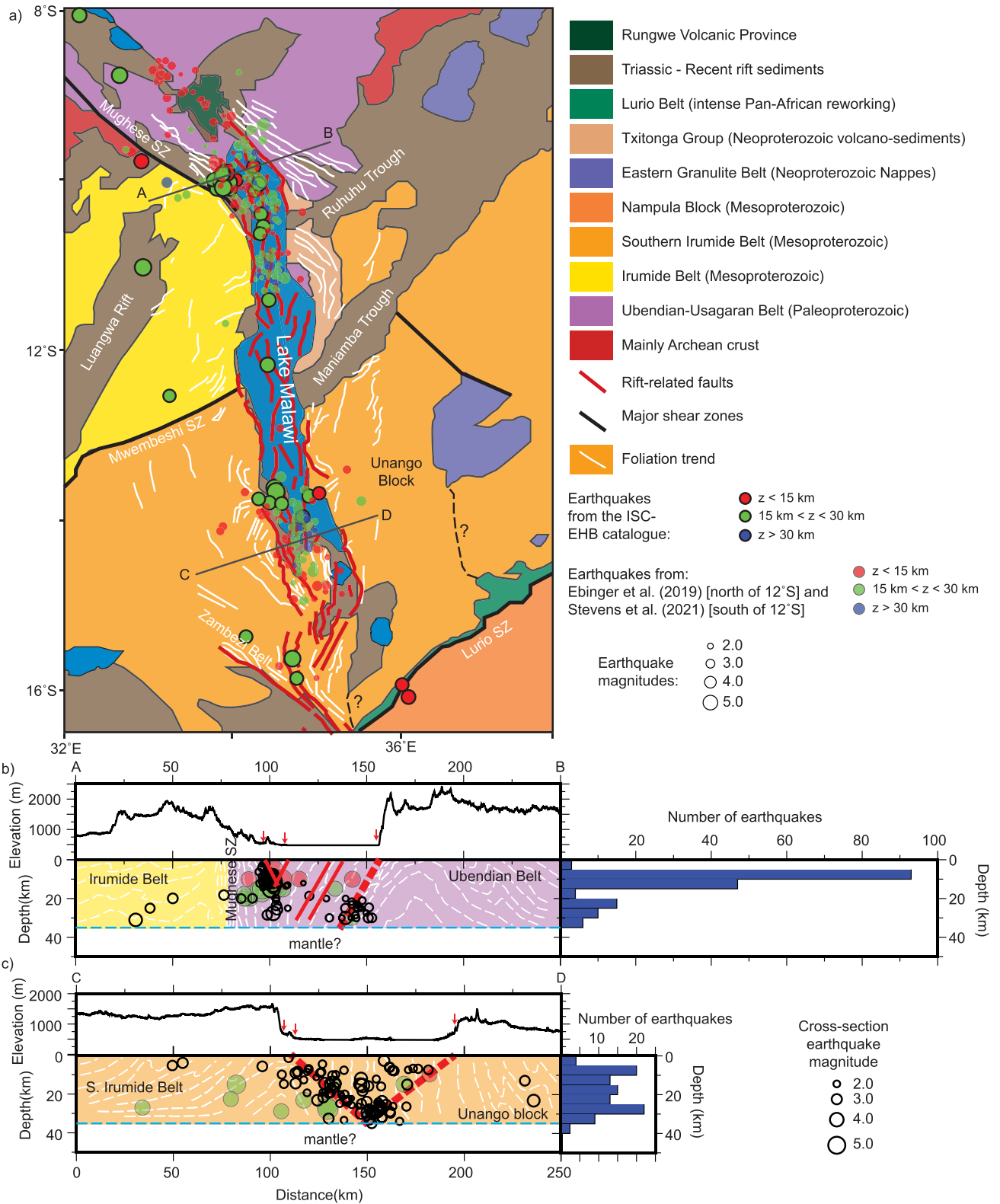


Figure 1.

This faulting and the associated intrusive events may have led to some local upper-crustal hydration and lower-crustal partial melting, but no wholesale rehydration or reworking of the lower crust comparable to the Proterozoic events.

## 2.2. Current Rifting

The Malawi Rift is considered juvenile as there is no surface expression of magmatism, the faults (although long) have relatively minor displacements of no more than a few kilometers (Carpenter et al., 2022; Ebinger et al., 1987; Mortimer et al., 2016; Ojo et al., 2022), and the total stretching is estimated at less than 10% (Sun et al., 2021). South of Lake Malawi, relatively well-exposed fault zones have damage zones that are typically less than 120 m thick, well below global trends for their length and indicating a very early stage of faulting (Carpenter et al., 2022; Williams et al., 2022a). Crustal thickness is typically in the range of 38–42 km, but there is evidence for localized crustal thinning by up to a few kilometers in the center of the Rift (Hopper et al., 2020; Wang et al., 2019). The lithospheric mantle, however, appears to have experienced more thinning, and may be upwarped by tens of kilometers under the rift axis—requiring thermal and/or chemical alteration in addition to mechanical thinning in the mantle (Hopper et al., 2020). Based on low  $V_p/V_s$  derived from receiver functions (Sun et al., 2021), there may be very minor melt proportions present in the rift axis. These data cannot identify the source of this minor melt, but the average shear velocity and Poisson's ratio in terranes flanking the rift imply that any crustal thinning and partial melting is localized within the rift center (Borrego et al., 2018). The same studies are consistent with a felsic to intermediate bulk composition of the crust hosting the Rift. The surface geology therefore seems representative of the crust as a whole—also consistent with the lower-crustal metamorphic conditions that were experienced by the current surface rocks. An exception is that a layer of mafic rocks may be present at the base of the crust (Albaric et al., 2009; Shudofsky et al., 1987), although this is suggested to be at most a few km thick (Julià et al., 2005; Kachingwe et al., 2015).

Current Rift-related deformation is expressed by  $2.2 \pm 0.3$  mm/year of approximately E-W extension (Wedmore et al., 2021). Earthquakes in Malawi are associated with dominantly normal-sense focal mechanisms (Craig et al., 2011; Ebinger et al., 2019; Williams et al., 2019), and the fault system is largely composed of faults with normal-sense displacements as determined from topographic expression, reflection seismology or aeromagnetic data (Williams et al., 2022c). Lower-crustal earthquakes have been recognized in the area for some time (e.g., Jackson & Blenkinsop, 1993; Nyblade & Langston, 1995), and recent local deployments have confirmed that seismicity spans the thickness of the crust (Figure 1; Ebinger et al., 2019; Stevens et al., 2021). The observed seismicity is not of sufficient cumulative moment to explain the geodetically determined strain (Ebinger et al., 2019), meaning that either elastic strain is accumulating on locked faults, or that there is a component of aseismic creep. Theoretically, if the  $\sim 100$  km-long normal faults ruptured along their entire length and through a seismogenic thickness equivalent to the whole crust, earthquake magnitudes could reach  $M_w 8$  (Hodge et al., 2020; Jackson & Blenkinsop, 1997; Williams et al., 2022b). On the other hand, the faults may rupture in smaller segments, producing smaller but more frequent events, as seen in the upper-crustal Karonga sequence of 2010 (Biggs et al., 2010; Fagereng, 2013). Where local seismic networks have been deployed and allow sufficiently precise earthquake locations to be obtained, the earthquakes dominantly localize onto fault systems along and under the rift axis (Figures 1b and 1c). At the southern end of Lake Malawi, a cluster of earthquakes were observed at the base of the seismogenic zone, between 30 and 35 km depth (possibly at and above the Moho—Figure 1c; Stevens et al., 2021). Around northern Lake Malawi, continued activity in the area of the Karonga earthquake swarm shows clustered, frequent earthquakes in the upper crust, related to extension in the hanging wall of the Livingstone Border Fault (Figure 1b; Biggs et al., 2010; Ebinger et al., 2019; Gaherty et al., 2019).

**Figure 1.** The geological and tectonic setting of the Malawi Rift. (a) Simplified geological map after Fritz et al. (2013) with active faults from Williams et al. (2022c) and location of earthquakes in instrumental time from the ISC-EHB catalog (1964–present; Engdahl et al., 2020) and local catalogs published by Ebinger et al. (2019) and Stevens et al. (2021). (b, c) Schematic geological cross-sections inspired by larger-scale interpretations in Fritz et al. (2013). Filled circles are earthquakes from the global ISC-EHB catalog, colored as in (a). These have location uncertainties exceeding 10 km. Open circles in (b) are earthquakes recorded in a local array by Ebinger et al. (2019), within 20 km of the cross-section line and located with  $<5$  km vertical and  $<1.2$  km horizontal uncertainty. Open circles in (c) are earthquakes recorded in a local array by Stevens et al. (2021), within 100 km of the cross-section line and located with  $<5$  km vertical uncertainty. Topography from SRTM30 outlines the rift valley, and the surface expression of major faults are shown with red arrows. In (b) the Livingstone Border Fault is extrapolated to depth with a  $60^\circ$  dipping thick dashed red line, and hanging wall faults are extrapolated with thinner red lines also at  $60^\circ$  dip. In (c), border fault systems on both sides of the Lake are extrapolated with dips  $<60^\circ$  following Stevens et al. (2021). Histograms show depth distribution of the local earthquakes shown in the cross-sections. SZ, shear zone.

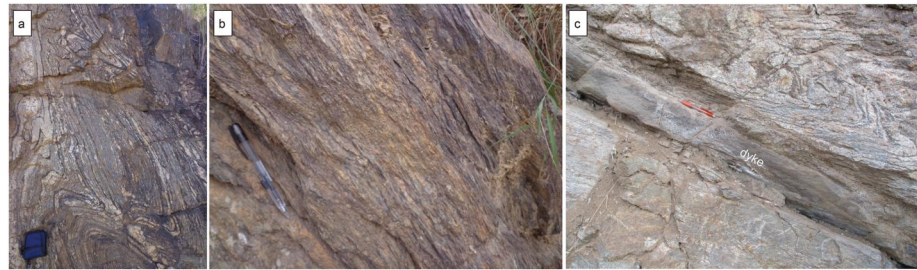


**Figure 2.** Photographs illustrating examples of inherited metamorphic fabrics in the currently rifting, Proterozoic basement rocks in Malawi: (a) migmatitic fabric and (b) foliated quartz-feldspar-biotite gneiss, both near the Mughese shear zone at the northwest shore of Lake Malawi, and (c) a fine-grained dyke reactivated as a shear zone, near the Thyolo fault in south Malawi.

Lower-crustal seismicity, however, occurs below these events, as well as in the lower crust below the surface expression of the Livingstone Border Fault (Figure 1b; Ebinger et al., 2019).

### 2.3. Conditions and Setting of Lower-Crustal Seismicity

To discuss the conditions of lower-crustal earthquakes in Malawi, we constructed a 1-D thermal gradient for the continental crust, assuming conductive heat transfer:

$$T(z) = T_0 + \left(\frac{Q_m z}{k}\right) + \left(\frac{(Q_0 - Q_m) h_r}{k}\right) \left(1 - \exp\left(\frac{-z}{h_r}\right)\right) \quad (1)$$

where  $T_0$  is the surface temperature (20°C),  $z$  is depth,  $Q_m$  is heat flow at the base of the model,  $Q_0$  is heat flow at the surface,  $k$  is the coefficient of thermal conductivity and  $h_r$  is the length scale for the depth-decay of radiogenic heat production.

We set  $Q_m = 30 \text{ mW/m}^2$ , slightly warmer than observed on average in stable continental regions (Mareschal & Jaupart, 2013) to reflect some increase in heatflow below the active rift, and  $k$  to a typical continental crust value of  $2.5 \text{ W/m/K}$  (Clauser & Huenges, 1995; Petitjean et al., 2006). The value of  $h_r$  is uncertain. The upper bound is that  $h_r$  equals crustal thickness, assuming the bulk of radiogenic elements are distributed evenly throughout the crust, but given that old, depleted crust generally has relatively low heat production (Jaupart et al., 2016), this is unrealistic in the East African context away from relatively recent intrusions. We set  $h_r$  to 10 km, which is the thickness of the quartz-dominated upper crust in the preferred model of Nyblade and Langston (1995), and reflects the presence of some upper-crustal sedimentary basins and recent intrusions within a generally depleted crustal block. We bracket the likely thermal conditions between two gradients representing the range of heat flow values calculated from aeromagnetic data by Njinju et al. (2019b). The cooler bound is  $Q_0 = 60 \text{ mW/m}^2$ , which is representative of the Precambrian basement away from hot springs, and the warmer bound assumes  $Q_0 = 80 \text{ mW/m}^2$ , which is representative of Karoo-age sedimentary basins (Njinju et al., 2019b). Using these values as surface heat flow, our model predicts thermal gradients between approximately 10 and  $15^\circ\text{C/km}$  for the crust in the rift region (Figure 3). Although cold for continental crust in general and continental rifts in particular, these gradients give temperatures of  $400\text{--}600^\circ\text{C}$  at the Moho, consistent with Moho temperatures calculated for other regions with active seismicity in quartzofeldspathic to feldspathic lower crust (McKenzie et al., 2005). We note that Njinju et al. (2019b) calculate higher thermal gradients,  $22\text{--}32^\circ\text{C/km}$ , based on an assumption of a linear thermal gradient. Directly measured surface heat flow in Lake Malawi, however, is typically  $<80 \text{ mW/m}^2$  with only a few examples of locally higher values that likely relate to hydrothermal flow along faults (Jones, 2020; Von Herzen & Vacquier, 1967), such that we consider  $<80 \text{ mW/m}^2$  a reasonable upper bound for regional surface heat flow, and thus that our non-linear regional thermal gradients are reasonable given the parameter choices outlined above.

The reason for the relatively deep seismicity remains debated. It may be a consequence of cold and dry crust (Craig & Jackson, 2021), but this requires very high stresses that are difficult to reconcile in this setting without invoking an additional weakening mechanism such as fluids or local, weak, high strain rate zones (Fagereng, 2013). A suggestion for local weakening is that mantle-derived fluids infiltrate the lower crust, as proposed along the extension of the rift in Botswana (Gardonio et al., 2018), although it is unclear how such fluids may

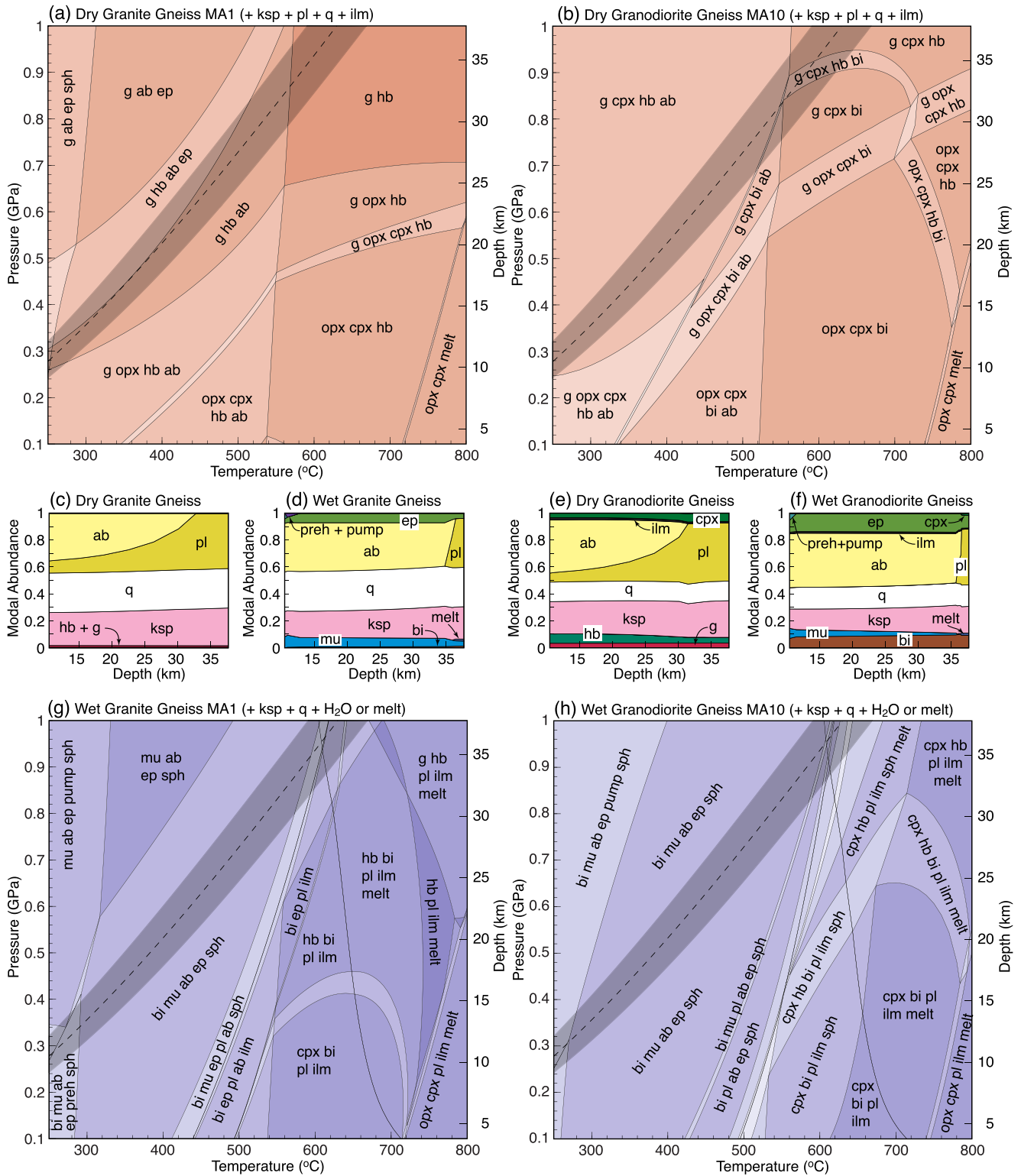


Figure 3.

migrate into the lower crust. The model suggested for lower-crustal earthquakes in Indian lithosphere colliding with the Himalayas invokes upper-crustal seismicity as a source for lower-crustal stress transients (Jamtveit et al., 2018). While this may be relevant for some aftershocks from the 2009 Karonga sequence (Biggs et al., 2010; Gaherty et al., 2019) or the 1989 Salima earthquake (Jackson & Blenkinsop, 1993), small earthquakes without known associated upper-crustal main shocks are present throughout the Malawi crust (Ebinger et al., 2019; Stevens et al., 2021; Figures 1b and 1c), and the Salima earthquake itself likely initiated at >30 km depth with no known earlier upper-crustal events of note (Jackson & Blenkinsop, 1993). Inherited weaknesses due to pre-existing structures are potentially important, but we emphasize that such structures are typical of high grade metamorphic rocks, and include migmatites (Figure 2a), local viscous shear zones defined by foliated, finer-grained crystals of minerals with average, rather than low, friction (such as quartz and feldspar; Figure 2b) and shear zones localized on fine-grained dykes (Figure 2c). Although structures like these might localize viscous shear at lower-crustal temperatures and slow strain rates (c.f. Pennacchioni & Mancktelow, 2007), they are not frictionally weak (Hellebrekers et al., 2019). Where studied in detail, faults in Malawi appear to follow foliations locally where reasonably well—but not optimally—oriented for reactivation, and cross-cut them elsewhere (Hodge et al., 2018; Wedmore et al., 2020; Williams et al., 2019). A potential model is that shear zones localize viscous deformation in the mid- to lower crust, and thus have some control on the orientation of overlying faults (Dawson et al., 2018; Hodge et al., 2018; Kolawole et al., 2018; Wedmore et al., 2020); what Samsu et al. (2023) suggests referring to as “soft-linked structural inheritance.” Next we will quantify the metamorphic preconditioning of Malawi lower-crustal rocks, which will allow a discussion on possible weakening mechanisms and their requirements.

### 3. Mineral Equilibrium Modeling

#### 3.1. Methodology and Assumptions

Mineral equilibrium calculations are performed using the program THERMOCALC version 3.50 beta (Powell & Holland, 1988, updated December 2019) and an updated version of the internally consistent data set of Holland and Powell (2011, data set file tc-ds62.txt, created May 2013). Calculations were performed in the Na<sub>2</sub>O–CaO–K<sub>2</sub>O–FeO–MgO–Al<sub>2</sub>O<sub>3</sub>–SiO<sub>2</sub>–H<sub>2</sub>O–TiO<sub>2</sub>–O chemical system, and the activity–composition relations used are those of Green et al. (2016) and White et al. (2014). Regional mapping (Geological Survey of Malawi, 1966) and geophysical studies (Borrego et al., 2018) suggest that felsic to intermediate rocks dominate the crust in Malawi, and two bulk-rock compositions reported by Kröner et al. (2001) were selected to represent felsic and intermediate end-members that bracket the likely range of rock compositions occurring in the seismogenic zone. The potential presence of younger felsic and alkaline igneous rocks such as the Chilwa Province is unlikely to affect our results, as their composition, mineralogy and fluid content are similar to that of the chosen felsic end-member. Sample MA1 is a biotite gneiss interpreted to be from a granitic protolith, whereas sample MA10 is a biotite-hornblende gneiss derived from a granodioritic protolith (Kröner et al., 2001). The measured compositions were converted to the model chemical system by disregarding minor amounts of P<sub>2</sub>O<sub>5</sub> and MnO (each <0.5 wt%), with the amounts of FeO and Fe<sub>2</sub>O<sub>3</sub> included as they are reported in Kröner et al. (2001).

In the modeling of high-grade metamorphic rocks that have experienced migmatization and melt loss, the bulk rock H<sub>2</sub>O content used in the modeling is chosen such that it allows the preserved metamorphic mineral assemblage to coexist with a minimal amount of melt (e.g., Diener et al., 2008; White et al., 2004). This mimics the situation after final melt loss at peak metamorphic conditions, when the assemblage would have coexisted with the last vestiges of melt (e.g., Diener et al., 2008; White et al., 2004). The pseudosection calculated for this composition and H<sub>2</sub>O content is appropriate for investigating the peak and retrograde metamorphic history, which in this instance encompasses the Proterozoic to modern evolution of the Malawi crust. For these calculations, the H<sub>2</sub>O content of samples MA1 and MA10 were taken to be 0.04 and 0.2 mol%, respectively. In addition,

**Figure 3.** Calculated pseudosections and mineral abundance diagrams for granite gneiss sample MA1 (left column) and granodiorite gneiss sample MA10 (right column). (a, b) Pseudosections for dry and residual bulk compositions with low H<sub>2</sub>O content. (c–f) Mineral abundances for dry and wet compositions calculated along the 70 mW/m<sup>2</sup> geotherm. (g, h) Pseudosections for wet, water-saturated bulk compositions. The dashed line and gray envelope denotes the 70 ± 10 mW/m<sup>2</sup> geotherm. Mineral abbreviations: ab, albite; bi, biotite; cpx, diopside clinopyroxene; ep, epidote; g, garnet; H<sub>2</sub>O, aqueous fluid; hb, hornblende; ilm, ilmenite; ksp, K feldspar; melt, silicate melt; mu, muscovite; opx, orthopyroxene; pl, plagioclase; preh, prehnite; pump, pumpellyite; q, quartz; sph, titanite.

calculations were also performed for fluid-saturated versions of these samples to simulate the effects of potential fluid addition at the current conditions of rifting.

### 3.2. Dry Compositions

Calculated pseudosections for samples MA1 and MA10 with a dry and residual fluid content are presented in Figures 3a and 3b. Both rock types predominantly consist of quartz and feldspars over the entire  $P$ - $T$  range considered, and also show somewhat similar topologies for their overall mineral assemblages. Melt-bearing two-pyroxene assemblages are present at the high- $T$ -low- $P$  conditions of Proterozoic peak metamorphism (Karamakar & Schenk, 2016; Kröner et al., 2001; Ring et al., 1997). The samples are calculated to consist of similar melt-absent two-pyroxene assemblages at medium- to high- $T$  and low- to medium- $P$  conditions (Figures 3a and 3b). Garnet is present at lower  $T$  and higher  $P$ , and is introduced at the expense of ortho- and/or clinopyroxene, whereas albite is present at  $T$  below  $\sim 500^{\circ}\text{C}$  (Figures 3a and 3b).

Along the calculated thermal gradient relevant to current rifting, both rock types are predicted to consist predominantly of quartz, K-feldspar, albite and plagioclase, with only very minor amounts of hornblende, garnet and clinopyroxene present (Figures 3c and 3e). The granite gneiss is calculated to consist of 30% quartz, 25%–28% K-feldspar, 40%–45% plagioclase + albite and less than 2% hornblende + garnet (Figure 3c). The granodiorite gneiss contains less quartz and more ferromagnesian minerals, and consists of 15% quartz, 24%–27% K-feldspar, 43%–45% plagioclase + albite, 3% hornblende, 4%–7% garnet and 3%–6% clinopyroxene (Figure 3e). The only mineralogical change that occurs with depth in either sample is a gradual increase in the abundance of plagioclase at the expense of albite, such that albite is not present at depths below 30 km (Figures 3c and 3e). No partial melting is predicted unless temperatures are well above  $800^{\circ}\text{C}$  at the base of the crust (Figures 3a and 3b), exceeding predictions by both our inferred geotherm and those by Njinju et al. (2019b).

### 3.3. Fluid-Saturated Compositions

Fluid-saturated pseudosections for samples MA1 and MA10 are presented in Figures 3g and 3h. Compared to the dry compositions presented above, the higher fluid content in these versions allows a variety of hydrous minerals to be stable. At  $T$  below  $\sim 500^{\circ}\text{C}$  both rock types consist of muscovite–biotite–epidote–albite-bearing assemblages, whereas they contain hornblende–clinopyroxene–biotite–plagioclase-bearing assemblages at  $T$  above  $\sim 550^{\circ}\text{C}$  (Figures 3g and 3h). Prehnite or pumpellyite are stable at  $T$  below  $300^{\circ}\text{C}$ , and both samples also become melt-bearing at  $T$  above  $600$ – $700^{\circ}\text{C}$  (Figures 3g and 3h).

Much like the dry compositions, the fluid-saturated versions of both rock types are calculated to consist predominantly of quartz, K-feldspar and albite for most depths along the inferred thermal gradient of current rifting (Figures 3d and 3f). The fluid-saturated granite gneiss contains 30% quartz, 18%–24% K-feldspar and 36% albite or plagioclase along with 4%–8% muscovite, 4% epidote and minor biotite ( $<1\%$ ; Figure 3d). The fluid-saturated granodiorite gneiss consists of 16% quartz, 15%–20% K-feldspar and 38%–41% albite or plagioclase along with 0%–7% muscovite, 9% epidote and 7%–9% biotite (Figure 3f). In both samples, epidote is replaced by prehnite and pumpellyite at depths of less than  $\sim 10$  km, whereas albite transforms to plagioclase at a depth of 35 km (Figures 3d and 3f). Minor melt ( $\sim 1\%$ ) is introduced at depths in excess of 35 km in both rock types.

## 4. Lower Crust Rheology

We combine inferred and calculated  $P$ - $T$  conditions, compositions, and rheological models to describe a model for the strength evolution of the crust from the end of the Pan-African metamorphic event to current rifting (Figure 4). The thermodynamic models indicate that felsic to intermediate crustal rocks in the rift are essentially quartzofeldspathic, with 15%–30% quartz and the rest a mixture of feldspars. Rheologically, K-feldspar, albite, and plagioclase behave similarly in that they are relatively strong when coarse grained and dry, but weaken significantly at small grain size or high water content (e.g., J. Chen et al., 2021; Rybacki & Dresen, 2004), and we thus group them together, and model bulk rock rheology as a two-phase quartz–feldspar mixture. We follow Handy et al. (1999) and consider two microstructural end-members: rocks with interconnected weak layers (IWL), essentially representing rocks with a well-oriented penetrative foliation such as in pre-existing shear zones; and rocks with a strong load-bearing framework (LBF), that is, rocks where any weak phases are randomly distributed and not interconnected in a foliation, approximating the majority of the crust outside of shear zones.

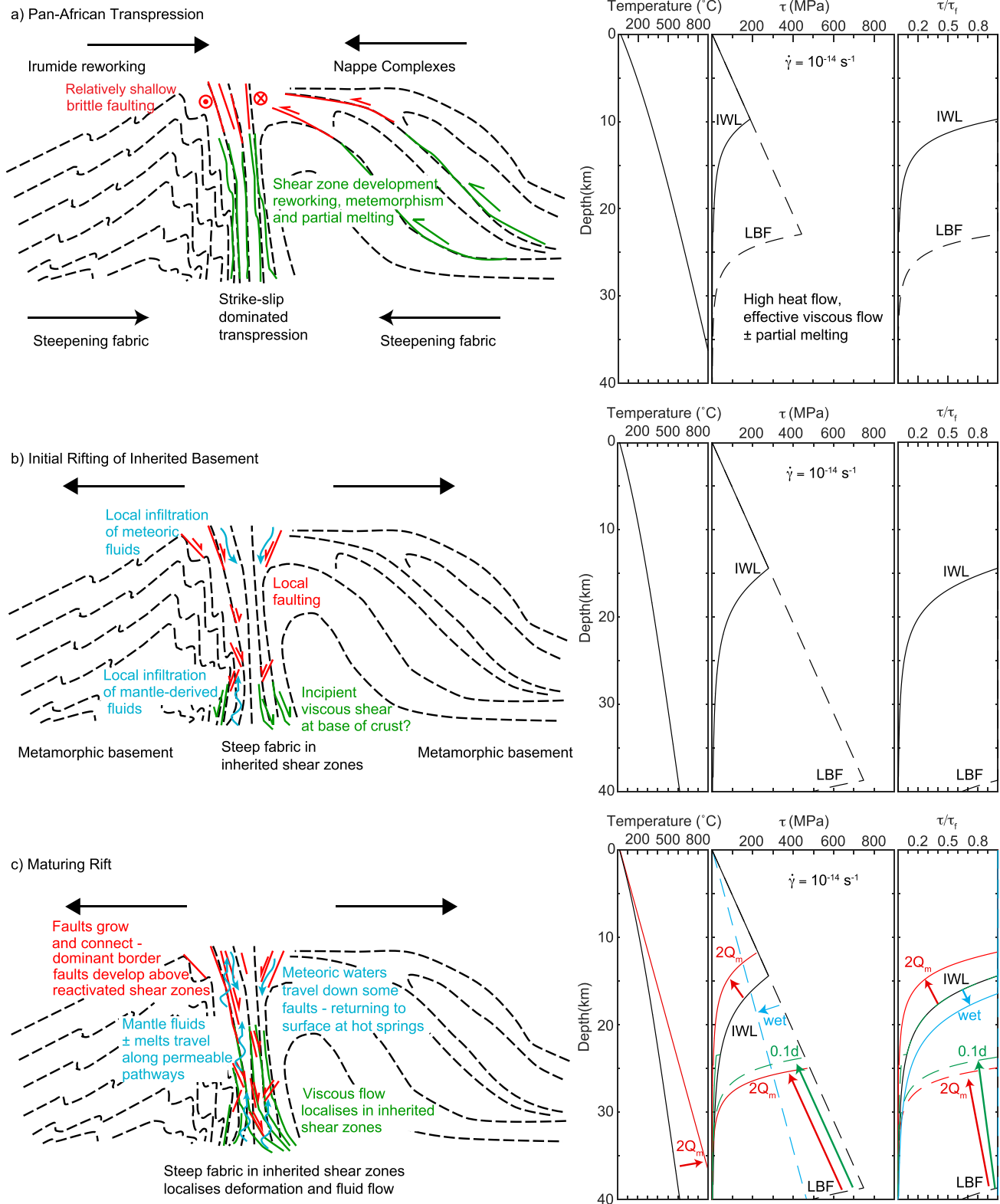


Figure 4.

This division into foliated and non-foliated rocks is consistent with the hypothesis that fabric formation is a dominant process localizing ductile shear (Montési, 2013).

#### 4.1. Methods and Assumptions to Calculate a Simplified Two-Phase Rheology

For strong LBF, the bulk strain-rate is controlled by the strain-rate of the strong framework and is therefore uniform. With this uniform strain-rate assumption the composite strength is simply the volumetrically weighted sum of the component strengths, representing an upper-bound on bulk strength:

$$\tau_{LBF} = \tau_w \phi_w + \tau_s (1 - \phi_w) \quad (2)$$

In this equation,  $\tau$  is shear strengths of the weaker (subscript  $w$ ) and stronger (subscript  $s$ ) of the two phases, and  $\phi_w$  is the volume fraction of the weaker phase. For viscously deforming rocks, the shear strength is given by:

$$\tau_v = \sqrt[n]{\frac{Q + PV}{RT} + \ln\left(\frac{\dot{\gamma} d^p}{3^{(n+1)/2} A f_{H_2O}^m}\right)} \quad (3)$$

where  $Q$  is activation energy,  $P$  is pressure,  $V$  is activation volume,  $R$  is the universal gas constant,  $T$  is temperature in Kelvin,  $\dot{\gamma}$  is strain-rate in the mineral phase,  $d$  is grain size,  $A$  is an empirical parameter that depends on composition and deformation mechanism,  $f_{H_2O}$  is water fugacity, and  $m$ ,  $n$ , and  $p$  are exponents that primarily depend on the deformation mechanism. We use parameters from Lu and Jiang (2019) for quartz deformation, which we assume to occur by dislocation creep, and from Rybacki and Dresen (2000) for feldspar deformation, where we use the lowest flow stress from their dislocation and diffusion creep flow laws. We approximate  $f_{H_2O}$  as a function of  $P$  and  $T$  following Shinevar et al. (2015). We assume grain size is 1 mm, on the smaller end for crystalline rocks and as such potentially underestimating viscous strength in feldspars deforming by diffusion creep.

In the case of IWL microstructure, strain is localized within the weaker phase and strain-rate is not uniform (Handy, 1994; Handy et al., 1999). Instead, the strain-rate in the weak phase is elevated and becomes (Handy, 1994):

$$\dot{\gamma}_w = \dot{\gamma} \phi_w^{(1/\tau_c)-1} \quad (4)$$

where  $\tau_c$  is the strength contrast  $\tau_s/\tau_w$  at bulk strain rate  $\dot{\gamma}$ . In contrast, the strain rate in the strong phase is reduced relative to the bulk strain rate, and given by (Handy, 1994):

$$\dot{\gamma}_s = \dot{\gamma} \frac{1 - \phi_w^{(1/\tau_c)}}{1 - \phi_w} \quad (5)$$

Using these mineral phase strain rates, the bulk stress of a rock with IWL becomes (Handy, 1994):

$$\tau_{IWL} = \tau_w \phi_w^{(1/\tau_c)} + \tau_s (1 - \phi_w^{(1/\tau_c)}) \quad (6)$$

We use the same viscous deformation parameters for IWL microstructures as we did for LBF. In other words, we assume composition and grain size are the same, and the only difference is the presence and absence of an interconnected fabric. This will underestimate the relative strength reduction within shear zones, relative to where any grain size reduction or localization into compositionally controlled weaknesses have occurred.

**Figure 4.** Schematic cartoon cross-sections of (a) metamorphic and structural pre-conditioning of the Malawi Rift, (b) rift initiation, and (c) rift maturation. For each stage, we also estimate the depth-dependence of temperature, shear strength, and the ratio of bulk shear strength ( $\tau$ ) to frictional yield strength ( $\tau_f$ ). In the strength plots, IWL, interconnected weak layers (solid lines) and LBF, strong load-bearing framework (dashed lines). For strength of the maturing rift, the red lines show the effect of doubling the basal heat flow ( $Q_m$ ), the green lines the effect of reducing grain size by an order of magnitude ( $0.1d$ ), and the blue lines of changing from dry to hydrostatic fluid pressure. See the text for further details.

Following Handy et al. (1999) we also allow for the strong phase to be brittle, if the modified Navier-Coulomb criterion for frictional sliding along well-oriented fractures gives a strength that is lower than the viscous flow strength at a given strain rate. The strength of the relevant phase is then (Jaeger et al., 2007):

$$\tau_f = 0.5[a + P(1 - \lambda)(b - 1)] \sin(90^\circ - \tan^{-1} \mu) \quad (7)$$

where  $\lambda$  is the ratio of pore fluid pressure ( $P_f$ ) to lithostatic pressure,  $\mu$  is friction coefficient,  $b = (\sqrt{1 + \mu^2} - \mu)^{-2}$ , and  $a = 2C_0\sqrt{b}$  where  $C_0$  is cohesive strength (shear strength at zero normal stress). For our quartzofeldspathic rocks, we take typical “Byerlee” values of  $C_0 = 50$  MPa and  $\mu = 0.6$  (Byerlee, 1978).

#### 4.2. Calculated Rheological Evolution

We first consider the rheology of the crust at the end of Pan-African transpression in Malawi. We fit a continental thermal gradient to the estimated  $P$ - $T$  conditions of  $\sim 900^\circ\text{C}$  at 35 km depth (Figure 4a), noting that some estimates are warmer than this. This is a substantially warmer crust than we estimate for current rifting, but consistent with high heat flow in active collisional margins today (e.g., Jaupart et al., 2016), for example, as a result of advection and crustal thickening. It is also consistent with observation of migmatitic textures implying partial melting of lower-crustal rocks now exhumed to the surface in the Malawi Rift (Figure 2a). The rheological structure of crust with IWL and consisting of 20% quartz and 80% feldspars with this thermal gradient involves a 10 km thick brittle layer with a peak strength of  $\sim 200$  MPa above a thick, viscous, weak, lower crust (Figure 4a). Conversely, the frictional-viscous transition may be nearer 25 km deep if the crust is approximated to be intact and contain a feldspar LBF. We highlight that irrespective of microstructure, flow strength at depths deeper than 25 km were likely very low:  $<100$  MPa, and only a few MPa in shear zones, and even weaker in the presence of melt. This would have promoted development of steeply dipping foliations within the transpressional shear zones that formed at the time (Tikoff & Teysier, 1994).

Initiation of the current rift would have occurred in crust that inherited the composition and structure developed by the end of the Pan-African transpression (Figure 4b), but the intervening period of little tectonic activity would have led to a cooler geotherm, as reflected by the relatively low current heat flow (Njinju et al., 2019b). Early rifting processes also occurred locally in the Karoo and Cretaceous extensional events (Castaing, 1991), but like current rifting, in crust with characteristics inherited from Proterozoic deformation and metamorphism. The effect on strength, retaining a composition of 20% quartz and 80% feldspars, with any weaker minerals removed by previous metamorphic reactions, is that crust approximated as IWL is brittle to a depth of  $\sim 15$  km, with a peak strength of  $\sim 250$  MPa. Approximated as LBF, the crust is strong, brittle, and potentially seismogenic to nearly 40 km depth, with a peak strength exceeding 700 MPa (Figure 4b). In this interpretation of the current rift, there may be viscously deforming weak zones present throughout the lower crust, but these are embedded in much stronger, brittle crust where viscous deformation is difficult because temperatures are low, and the rocks are coarse-grained and enriched in relatively strong, residual minerals. The same interpretation applies to Karoo and Cretaceous rifting episodes.

In a more mature rift—where crustal thinning is occurring and heat flow at the base of the crust has increased (Figure 4c)—the rocks are brittle to shallower depths and viscous yield strength is lower. Doubling  $Q_m$  to simulate mantle upwelling moves the frictional-viscous transition to 12 km depth in weak IWL crust, and 25 km in strong LBF crust (Figure 4c). Peak strength reduces to  $\sim 200$  MPa for IWL crust and  $\sim 500$  MPa for LBF crust. Another possible effect of progressive crustal extension is a reduction in grain size that allows weakening, particularly of feldspars that control strength of LBF microstructures (quartz is weak anyway), through a switch from dislocation to diffusion creep (Figure 4c). Ruh et al. (2022) recently suggested such grain-size reduction as a dominant process initiating continental rifting. Introduction of melt or other fluids into the lower crust may also lead to weakening in several ways: the frictional resistance may be reduced by increased fluid pressure, or viscous flow strength can be reduced by fluid-assisted dissolution-precipitation creep (a more efficient form of diffusion creep), or by allowing retrograde reactions that increase the amount of weaker hydrous minerals (Figure 3). Going from dry faults to a hydrostatic fluid pressure regime with a grain-boundary fluid present reduces the peak strength in IWL crust to  $\sim 150$  MPa, and allows brittle deformation in LBF crust at shear stresses  $<450$  MPa (Figure 4c). This is an overestimate of strength as we do not include effects of minor proportions of new, hydrous minerals that may grow with addition of water (Figure 3). Note that other than increasing fluid pressure, all these

weakening mechanisms promote viscous creep and lead to shallowing of the frictional-viscous transition. These plots assume rifting dominated by tectonic faulting; substantial, further weakening than what is shown here is possible with increased melting and transition to magmatic rifting (Buck, 2004).

In Figure 4 we have also plotted bulk shear strength,  $\tau$ , versus the frictional yield strength  $\tau_f$ . This plot illustrates the potential for frictional slip and generation of earthquakes. A ratio of 1 indicates that frictional sliding is the easiest and therefore preferred mechanism, while values approaching zero imply that viscous creep is dominant, and there is unlikely to be any accumulation of elastic strain (because of very efficient creep). Intermediate values imply that although bulk viscous creep is easier than frictional sliding, elevated stresses in higher-strength materials, such as lenses of intact LBF crust in anastomosing IWL shear zones, may lead to local frictional failure (Beall et al., 2019; Fagereng & Beall, 2021). These plots therefore indicate the possibility of the whole crust being seismogenic at current conditions if it is approximated as a dry or wet LBF ( $\tau/\tau_f = 1$ ), or the lower crust being completely aseismic and viscous if it is approximated as comprising only IWL ( $\tau/\tau_f \rightarrow 0$ ).

## 5. Discussion

The Malawi Rift is localized in—and propagates through—granitic and granodioritic gneisses that experienced high- $T$  metamorphism during one or more orogenic events during the Proterozoic (De Waele & Mapani, 2002; Fritz et al., 2013; Karamakar & Schenk, 2016; Kröner et al., 2001; Manda et al., 2019; Ring et al., 1997). As such, the Malawi crust has a metamorphic inheritance that may explain both (a) how the rift is able to propagate through seemingly too strong, thick crust and lithosphere (Kendall & Lithgow-Bertelloni, 2016), and (b) the occurrence of deep-crustal earthquakes (Ebinger et al., 2019; Nyblade & Langston, 1995; Stevens et al., 2021).

### 5.1. Composition and Rheology of Rifting Malawi Crust

Mineral equilibrium calculations show that rocks at mid- to lower-crustal depths throughout the Rift consist largely of quartz and feldspars, with very minor amounts of garnet, pyroxene or amphibole (Figures 3c and 3e). Notably, these rocks contain almost no hydrous minerals, and are modeled to be completely free of phyllosilicates. Such rocks are likely to have medium- to coarse-grained equigranular textures and only weakly developed penetrative fabrics away from high-strain zones, and are approximated with a loadbearing framework (LBF) microstructure (Figure 4). Such rocks will preferentially undergo frictional failure and are calculated to be potentially seismogenic at all depths below the Rift at the inferred current geotherm (Figure 4b). On the scale of the Rift, inherited shear zones may impart a rheological anisotropy by being zones of more pervasive fabrics. Such IWL will decrease viscous shear resistance (Figure 4b), but have comparable frictional strength to surrounding rocks with lower inherited strain (Hellebrekers et al., 2019).

The observation that Malawi seismicity extends throughout the lower crust (Figure 1; Craig et al., 2011; Ebinger et al., 2019; Stevens et al., 2021) implies that dry and strong, quartzofeldspathic rocks occur at all crustal depths in and around the Malawi Rift. Our rheological models calculate the frictional-viscous transition in quartzofeldspathic rocks to occur at between 15 and 40 km depth with our assumed current Malawi thermal gradient (Figure 4b). Because the crust is uniformly frictionally strong, the shallower depth is associated with viscously weak shear zones, while the deeper estimate is appropriate for crust away from inherited, viscous weaknesses.

### 5.2. Conditions and Mechanisms of Fault Initiation and Propagation

Kendall and Lithgow-Bertelloni (2016) calculated that a driving stress of no more than 100 MPa is available for rifting of African lithosphere. As they concluded, our rheological models also show that the overall peak strength of rifting Malawi crust can only be that low in fine-grained, pre-existing viscous shear zones with an interconnected quartz or very fine-grained feldspar fabric (Figure 4). Frictional failure in the present-day strong, dry and isotropic crust requires substantially higher stresses. As such, the only way that the rift can continue to propagate is to predominantly reactivate pre-existing weak structures through viscous creep. This, however, does not account for the observed lower crustal seismicity, which needs to be explained by a separate mechanism. The current crust has been thoroughly dehydrated, such that internal fluid production cannot be a mechanism to allow seismicity (cf. Etheridge et al., 1984; Yardley, 1986). Fluids may be available from above (meteoric fluids) or below (mantle fluids), but these external fluids cannot be involved in initiating lower-crustal seismicity without first developing a permeability structure. Hot springs in the Malawi Rift imply some fluid flow along faults, but calculations based on silica and cation geothermometers show that the hot springs are fed by meteoric waters that

reached  $<200^{\circ}\text{C}$  (Dávalos-Elizondo et al., 2021), that is, did not interact with rocks at lower-crustal temperatures. The dry rocks are also not conducive to melting at current crustal temperatures without first adding fluids (Figures 3a and 3b), restricting potential for melt or melt-related fluids at depth. We therefore suggest that lower-crustal seismicity must initiate by an increase in stress or decrease in strength that does not require fluids.

Several studies have highlighted the spatial correlation between Malawi border faults and inherited shear zones (Dawson et al., 2018; Kolawole et al., 2018; Versfelt & Rosendahl, 1989; Wedmore et al., 2020; Wheeler & Rosendahl, 1994), although the faults do not necessarily reactivate the shear zone foliation (Hodge et al., 2018). Our rheological models imply that any weakness resides either near the surface where confining pressures are low, or at the base of the crust where inherited shear zones have low resistance to viscous flow. As rifting in Africa is essentially driven by mantle flow (Accardo et al., 2020; Hopper et al., 2020; Kendall & Lithgow-Bertelloni, 2016), it is most likely that current localized rifting initiated by reactivation of inherited shear zones in the viscous regime. Shear zones, however, tend to be tabular features of variably developed fabric (e.g., Carreras et al., 2010; Goodwin & Tikoff, 2002; Rennie et al., 2013), and therefore variable strength and rheological behavior (e.g., Druguet et al., 2009; Fagereng & Sibson, 2010). A mechanism for generating brittle failure at middle and lower-crustal depths is therefore by locally increasing driving stresses where anastomosing strands of viscous shear zones interact—exemplified by presence of pseudotachylyte in competent lenses within some exhumed Shear Zone networks (Campbell et al., 2020; Sibson, 1980). This requires the presence of viscously creeping shear zones, and implies that frictional sliding is a consequence of surrounding viscous creep. In this model, the lower crust must be accumulating (most) permanent finite strain viscously, and the cumulative seismic moment should be less than the geodetically determined strain. This is the case in Malawi (Ebinger et al., 2019), but the instrumental record is short relative to the potential repeat time of large earthquakes spanning the crust and may therefore underestimate the seismic moment (Williams et al., 2023). It is, however, also implicit that the size of lower crustal earthquakes will be limited by the length-scale of possible rupture areas, which if embedded in weak, viscously deforming shear zones may be unlikely to reach more than a few kilometers. The mid- to lower crustal M6.3 1989 Salima earthquake likely required a length scale of about 10 km (Jackson & Blenkinsop, 1993), showing that this length scale is possible at depths likely dominated by viscous deformation.

### 5.3. Conditions and Mechanisms of Ongoing Seismicity

In the above model, rifting initiates by viscous lower-crustal deformation localized to inherited shear zones. Locally, faults may develop in areas of stress magnification in stronger rocks (Beall et al., 2019; Campbell et al., 2020; Druguet et al., 2009), reflected by lower-crustal seismicity predominantly located within and/or around viscous shear zones (Figure 1). Viscous shear may also trigger fault development in overlying upper crust, as shown elsewhere by evidence for increases in viscous shear zone strain rate driving clusters of upper crustal earthquakes in California and central Italy (Dolan et al., 2007; Mildon et al., 2022). Once a fault has formed, then if it is permeable and connected to an external fluid source, fluid may be introduced to the deep crust. There are a number of potential sources for such fluids. The closest source to the lower crust is the lithospheric mantle, which could contain metasomatic fluids from upwelling, deeper asthenosphere (Njinju et al., 2019a), or partial melts originating from small zones capable of decompression melting, for example, by being more hydrated or compositionally more fertile (Hopper et al., 2020). Rapid stressing by melt infiltration from the mantle has been suggested to drive seismicity in ductilely deforming lower crust beneath southern Tanganyika, where crustal thinning has locally reached  $\sim 20\%$  (Hodgson et al., 2017; Lavayssi re et al., 2019).  $\text{CO}_2$ -rich fluids originating from the mantle, for example, degassing related to partial melt, have been detected along faults penetrating the lower crust in the magmatic Eastern Branch of the East African Rift, including young ( $<7$  Ma) rift segments away from volcanoes (Lee et al., 2016; Muirhead et al., 2016). Fluid overpressure from  $\text{CO}_2$ -rich or aqueous fluids released above melt zones have also been invoked to explain earthquake swarms in the Rwenzori Mountains of Uganda (Lindenfeld et al., 2012), and at the eastern edge of the Tanzania Craton (Albaric et al., 2013).  $\text{CO}_2$ -rich, magma-derived fluids are therefore potentially important to trigger lower crustal seismicity, and localize strain along crustal-scale faults, if the faults are connected to actively melting mantle rocks. Finally, with sufficient permeability, a top-down system where meteoric waters reach the mid- to lower crust is also conceivable based on isotope studies in exhumed shear zones (Haines et al., 2016; Stenvall et al., 2020), although current hot springs in Malawi appear to be restricted to hydrothermal circulation at temperatures  $<200^{\circ}\text{C}$  (Dávalos-Elizondo et al., 2021).

Because the lower-crustal rocks are inherited from a higher-temperature regime they are metastable while dry, but several processes may initiate with the introduction of fluids. A key point, however, is that initial deformation at dry conditions are required to create a permeability pathway between the lower crust and the external fluid source, before these processes can activate. In some Malawi faults, this may have occurred already during Karoo or Cretaceous rifting episodes, which may have prepared some faults for easier reactivation during current rifting. Note, however, that a change from dominantly NW-NE extension direction in the Karoo (Castaing, 1991; Ring, 1995) to NE-SW to E-W in the current rift (Delvaux & Barth, 2010; Ebinger et al., 2019; Wedmore et al., 2021; Williams et al., 2019) potentially caused reactivation of differently oriented structures in these rift episodes. One fluid-driven process is the growth of hydrous retrograde minerals that are stable at the current  $P$ - $T$  conditions of rifting. Our results show that this mineral growth is not very dramatic, as the fluid-saturated assemblages of both the considered rock types are still dominated by quartz and feldspars, but with 5%–15% epidote forming at the expense of plagioclase and 7%–13% micas forming at the expense of K-feldspar (Figures 3c–3f). Whereas epidote is frictionally strong and relatively conducive to earthquake slip, growth of micas may cause substantial weakening and preference for aseismic creep (An et al., 2022; Fagereng & Ikari, 2020). The amount of retrograde mineral growth is more substantial in the granodioritic composition than the granite, but much less pronounced than in metasediments studied elsewhere (e.g., faults where retrograde phyllosilicate growth may potentially create interconnected weak faults; Fagereng & Diener, 2011; Imber et al., 1997). The retrograde rocks are also likely to be fine-grained and continued rifting will lead to increased lower-crustal temperatures as mantle upwelling and crustal thinning work in concert to increase basal heat flow. These processes lead to marked weakening, but also marked increased preference for viscous, aseismic deformation in the lower crust (Figure 4c).

Pressurization of fluids during prograde metamorphism can lead to brittle failure within otherwise viscously deforming regions (Chapman et al., 2022; Menegon & Fagereng, 2021; Yardley, 1986), which may explain seismicity at mid- and lower-crustal depths in compressional regimes. The Malawi crust, however, is too dry to produce local fluids, and any fluids introduced from an external source will first be consumed by growth of hydrous minerals as outlined above. As long as mineral growth keeps pace with fluid infiltration, fluid pressure will only be able to increase once these reactions are complete. Although the overall and long-term effect of fluid addition is viscous weakening and suppression of earthquakes at lower-crustal conditions, a transient, local effect may be a sufficient reduction in effective stress to trigger frictional failure (Figure 4c). This is enhanced by that stresses are already relatively low in rifting environments, and relatively minor increases in fluid pressure can be sufficient to switch the rheology from viscous to frictional (Figure 4c). The effect of these local, fluid-pressure-related earthquake triggers are, however, limited in size to the fluid-infiltrated area, and in time to when the lower crust is sufficiently strong to store elastic strain.

Overall, if permeability can be increased through re-activation of inherited, viscous shear zones where local seismicity is associated with stress risers, the influx of external fluids would provide a range of weakening mechanisms. These may initially promote local seismicity, but their long-term effect will be to increase ductility. Retrograde assemblages are typically finer-grained than the high-grade rocks, enhancing the rate of diffusion creep. The retrograde assemblage would also be somewhat (but not greatly) enriched in weaker phyllosilicates relative to the Proterozoic higher-grade metamorphic rock. Our modeling indicates that in cases of maximal hydration, the equilibrium assemblages only contain ~10% mica (Figure 3), which is unlikely to control the rheology as it is insufficient for an interconnected network. Weakening might also arise because dislocation creep is more efficient under hydrothermal conditions (Griggs & Blacic, 1965). These mechanisms would locally enhance viscous creep along local fluid pathways. This is not an earthquake mechanism, but a mechanism that may allow rifting to occur, dominantly by viscous mechanisms, in the crust above the potentially weakened lithospheric mantle under the Malawi Rift axis (Hopper et al., 2020). If the crust is only locally weak, perhaps along relatively thin, possibly anastomosing shear zones, then earthquakes could occur in the stronger rocks surrounded by these shear zones (Campbell et al., 2020), but would cease with increased viscous strain, fluid infiltration, and associated viscous weakening. The relatively juvenile and incipient nature of the Malawi Rift can therefore be a contributing factor in its propensity for deep seismicity compared to more mature rift segments.

It may be that some fault zones have already been sufficiently weakened to no longer produce much, if any, lower crustal seismicity; for example, some faults that have been repeatedly reactivated throughout the Karoo, Cretaceous, and current rifting events are good candidates for having developed permeability, retrograde, weak assemblages, and smaller grain size. The Mughese Shear Zone is one such candidate (Dawson et al., 2018; Kolawole et al., 2018), and indeed has little if any detected lower crustal seismicity along the section covered by

the deployment of Ebinger et al. (2019) (Figure 1b), although only a small part of the Mughese Shear Zone was covered, for a short part of an earthquake cycle. Conversely, the Livingstone Fault is a border fault with seismic activity throughout the crust (Ebinger et al., 2019; Figure 1b). Although it has a similar long history of deformation, this fault was likely first active as a strike-slip fault (Wheeler & Karson, 1989), perhaps like the similarly oriented Kanda fault in southern Tanzania, where a change from strike-slip to normal faulting is interpreted between Karoo and current rifting (Delvaux et al., 2012). While strike-slip faulting can create permeability, normal faulting occurs at lower shear stress, is prone to fluid-driven failure at lower pore pressure, and is generally more efficient at rehydrating the crust (c.f. Sibson, 2017). Consequently, we suggest that the subvertical Mughese Shear Zone with a longer history of normal faulting may have reached a more weakened state in the lower crust, whereas the crustal-wide seismogenic nature of the Livingstone Fault, as well as of the Bilila-Mtakataka Fault (Stevens et al., 2021; Figure 1c), reflects ongoing weakening of an overall more brittle and stronger feature. Further study of the Mughese Shear Zone and other major structures with large post-Pan African displacement may test this hypothesis.

## 6. Conclusions

The crust surrounding the Malawi Rift has experienced multiple granulite facies metamorphic events. Our mineral equilibrium modeling results, combined with estimates of peak  $P$ - $T$  conditions, indicate that metamorphism during the Proterozoic generated a crust that is thoroughly dehydrated and dominated by a quartz and feldspar assemblage that is metastable at current conditions. Along thermal gradients constrained by heat flow determined from aeromagnetic data, crustal temperatures are cool relative to those of Proterozoic metamorphism, and local melting is not predicted to occur without addition of water and/or heat from an external source. These results imply that strain is accommodated in the rift under fluid (melt and hydrous)-absent conditions except where an external fluid (melt, hydrous, or carbonaceous) may locally infiltrate once a permeability network has formed.

For rifting to be possible, low thermal gradients and a mechanically strong, dry quartzofeldspathic mineralogy demand localization of mid- to lower-crustal strain into viscously weakened, inherited shear zones, and for deformation to occur predominantly by aseismic viscous creep. These shear zones are embedded within high-strength crust, and interaction between creeping shear zones and strong blocks of enveloped or surrounding rocks may locally increase stress and trigger brittle failure, thereby allowing seismicity to occur at mid- to lower-crustal depths. Increased strain rate from shallower earthquakes can also trigger lower-crustal seismicity, as suggested in other tectonic settings; however, local deep seismicity in the absence of such events (Figure 1) indicates that these are not a prerequisite. We therefore suggest that during rifting of previously deformed and metamorphosed crust, major faults are most likely to grow from below, with their location and orientation prescribed by underlying inherited viscous shear zones. This is consistent with the location of Rift faults within, but not consistently parallel to, inherited shear zones that lack frictionally weak minerals. An implication of this model is that the lower-crustal seismicity is essentially an artifact of viscous deformation, and—importantly—not directly linked or related to upper-crustal seismicity except where representing aftershocks from upper crustal earthquakes. Therefore, even though there are earthquakes throughout the whole crust, only exceptional circumstances would allow a single crust-spanning earthquake because the stress heterogeneity between dominantly aseismic shear zones and faults governed by frictional strength is large.

## Data Availability Statement

This article does not use any new data. Earthquake catalogs used in Figure 1 are available through the original, referenced papers (Ebinger et al., 2019; Stevens et al., 2021). The THERMOCALC software and associated mineral thermodynamic models used for mineral equilibria calculations can be downloaded for free from: <https://hpxeosandthermocalc.org>, where relevant documentation is also available.

## References

- Accardo, N. J., Gaherty, J. B., Shillington, D. J., Hopper, E., Nyblade, A. A., Ebinger, C. J., et al. (2020). Thermochemical modification of the upper mantle beneath the northern Malawi Rift constrained from shear velocity imaging. *Geochemistry, Geophysics, Geosystems*, 21(6), e2019GC008843. <https://doi.org/10.1029/2019GC008843>
- Albaric, J., Déverchère, J., Perrot, J., Jakovlev, A., & Deschamps, A. (2013). Deep crustal earthquakes in North Tanzania, East Africa: Interplay between tectonic and magmatic processes in an incipient rift. *Geochemistry, Geophysics, Geosystems*, 15(2), 374–394. <https://doi.org/10.1002/2013GC005027>

## Acknowledgments

We appreciate many discussions with Juliet Biggs, Luke Wedmore and Jack Williams, who have all influenced the models presented here. We appreciate constructive reviews from Chris Morley and Rasheed Ajala, which significantly improved the paper. This work was supported by the EPSRC Global Challenges Research Fund (PREPARE project, Grant EP/P028233/1). Á. F. also acknowledges support from the project FricFrac funded by the Center for Advanced Study (CAS) at the Norwegian Academy of Science and Letters during academic year 2023–2024.

- Albaric, J., Déverchère, J., Petit, C., Perrot, J., & Le Gall, B. (2009). Crustal rheology and depth distribution of earthquakes: Insights from the central and southern East African Rift System. *Tectonophysics*, 468(1–4), 28–41. <https://doi.org/10.1016/j.tecto.2008.05.021>
- An, M., Zhang, F., Min, K.-B., Elsworth, D., He, C., & Zhao, L. (2022). Frictional stability of metamorphic epidote in granitoid faults under hydrothermal conditions and implications for injection-induced seismicity. *Journal of Geophysical Research: Solid Earth*, 127(3), e2021JB023136. <https://doi.org/10.1029/2021JB023136>
- Austrheim, H., & Boundy, T. (1994). Pseudotachylites generated during seismic faulting and eclogitization of the deep crust. *Science*, 265(5168), 82–83. <https://doi.org/10.1126/science.265.5168.82>
- Beall, A., Fagereng, A., & Ellis, S. (2019). Strength of strained two-phase mixtures: Application to rapid creep and stress amplification in subduction zone mélange. *Geophysical Research Letters*, 46(1), 169–178. <https://doi.org/10.1029/2018gl081252>
- Biggs, J., Nissen, E., Craig, T., Jackson, J., & Robinson, D. P. (2010). Breaking up the hanging wall of a rift-border fault: The 2009 Karonga earthquakes, Malawi. *Geophysical Research Letters*, 37(11), L11305. <https://doi.org/10.1029/2010GL043179>
- Bloomfield, K. (1961). The age of the Chilwa Alkaline Province. *Records of the Geological Survey of Malawi*, 1, 95–100.
- Borrego, D., Nyblade, A. A., Accardo, N. J., Gaherty, J. B., Ebinger, C. J., Shillington, D. J., et al. (2018). Crustal structure surrounding the northern Malawi Rift and beneath the Rungwe Volcanic Province, East Africa. *Geophysical Journal International*, 215(2), 1410–1426. <https://doi.org/10.1093/gji/ggy331>
- Brace, W. F., & Kohlstedt, D. L. (1980). Limits on lithospheric stress imposed by laboratory experiments. *Journal of Geophysical Research*, 85(B11), 6248–6252. <https://doi.org/10.1029/jb085ib11p06248>
- Brown, M. (1994). The generation, segregation, ascent and emplacement of granite magmas: The migmatite-to-crustally-derived granite connection in thickened orogens. *Earth-Science Reviews*, 36(1–2), 83–130. [https://doi.org/10.1016/0012-8252\(94\)90009-4](https://doi.org/10.1016/0012-8252(94)90009-4)
- Buck, W. R. (2004). Consequences of asthenospheric variability on continental rifting. In G. D. Karner, B. Taylor, N. W. Driscoll, & D. L. Kohlstedt (Eds.), *Rheology and deformation of the lithosphere at continental margins* (pp. 1–30). Columbia University Press. <https://doi.org/10.7312/karn12738-fm>
- Byerlee, J. (1978). Friction of rocks. In *Rock friction and earthquake prediction* (pp. 615–626). Springer.
- Camelbeeck, T., & Iranga, M. D. (1996). Deep crustal earthquakes and active faults along the Rukwa trough, eastern Africa. *Geophysical Journal International*, 124(2), 612–630. <https://doi.org/10.1111/j.1365-246X.1996.tb07040.x>
- Campbell, L. R., Menegon, L., Fagereng, A., & Pennacchioni, G. (2020). Earthquake nucleation in the lower crust by local stress amplification. *Nature Communications*, 11(1), 1–9. <https://doi.org/10.1038/s41467-020-15150-x>
- Carpenter, M., Williams, J. N., Fagereng, A., Wedmore, L. N. J., Biggs, J., Mphopo, F., et al. (2022). Comparing intrarift and border fault structure in the Malawi Rift: Implications for normal fault growth. *Journal of Structural Geology*, 165, 104761. <https://doi.org/10.1016/j.jsg.2022.104761>
- Carreras, J., Czeck, D. M., Druguet, E., & Hudleston, P. J. (2010). Structure and development of an anastomosing network of ductile shear zones. *Journal of Structural Geology*, 32(5), 656–666. <https://doi.org/10.1016/j.jsg.2010.03.013>
- Carter, G. S., & Bennet, J. D. (1973). *The geology and mineral resources of Malawi* (Bulletin No. 6). Geological Survey of Malawi.
- Castaing, C. (1991). Post-Pan-African tectonic evolution of South Malawi in relation to the Karoo and recent East African Rift Systems. *Tectonophysics*, 191(1–2), 55–73. [https://doi.org/10.1016/0040-1951\(91\)90232-h](https://doi.org/10.1016/0040-1951(91)90232-h)
- Catuneanu, O., Wopfner, H., Eriksson, P. G., Cairncross, B., Rubidge, B. S., Smith, R. M. H., & Hancock, P. J. (2005). The Karoo basins of south-central Africa. *Journal of African Earth Sciences*, 43(1–3), 211–253. <https://doi.org/10.1016/j.jafrearsci.2005.07.007>
- Chapman, T., Milan, L., & Vry, J. (2022). The role of metamorphic fluid in tectonic tremor along the Alpine Fault, New Zealand. *Geophysical Research Letters*, 49(2), e2021GL096415. <https://doi.org/10.1029/2021gl096415>
- Chen, J., Jin, Z., Liu, W., Wang, Y., & Zhang, J. (2021). Rheology of dry k-feldspar aggregates at high temperature and high pressure: An experimental study. *Tectonophysics*, 817, 229072. <https://doi.org/10.1016/j.tecto.2021.229072>
- Chen, W. P., & Molnar, P. (1983). Focal depths of intracontinental and intraplate earthquakes and their implications for the thermal and mechanical properties of the lithosphere. *Journal of Geophysical Research*, 88(B5), 4183–4214. <https://doi.org/10.1029/jb088ib05p04183>
- Clauser, C., & Huenges, E. (1995). Thermal conductivity of rocks and minerals. In *Rock physics and phase relations: A handbook of physical constants* (Vol. 3, pp. 105–126).
- Craig, T. J., & Jackson, J. A. (2021). Variations in the seismogenic thickness of East Africa. *Journal of Geophysical Research: Solid Earth*, 126(3), e2020JB020754. <https://doi.org/10.1029/2020jb020754>
- Craig, T. J., Jackson, J. A., Priestley, K., & McKenzie, D. (2011). Earthquake distribution patterns in Africa: Their relationship to variations in lithospheric and geological structure, and their rheological implications. *Geophysical Journal International*, 185(1), 403–434. <https://doi.org/10.1111/j.1365-246X.2011.04950.x>
- Dávalos-Elizondo, E., Atekwana, E. A., Atekwana, E. A., Tsokonombwe, G., & Laó-Dávila, D. A. (2021). Medium to low enthalpy geothermal reservoirs estimated from geothermometry and mixing models of hot springs along the Malawi Rift Zone. *Geothermics*, 89, 101963. <https://doi.org/10.1016/j.geothermics.2020.101963>
- Dawson, S. M., Laó-Dávila, D. A., Atekwana, E. A., & Abdelsalam, M. G. (2018). The influence of the Precambrian Mugheese Shear Zone structures on strain accommodation in the northern Malawi Rift. *Tectonophysics*, 722, 53–68. <https://doi.org/10.1016/j.tecto.2017.10.010>
- Delvaux, D., & Barth, A. (2010). African stress pattern from formal inversion of focal mechanism data. *Tectonophysics*, 482(1–4), 105–128. <https://doi.org/10.1016/j.tecto.2009.05.009>
- Delvaux, D., Kervyn, F., Macheyeke, A. S., & Temu, E. B. (2012). Geodynamic significance of the TRM segment in the East African Rift (W-Tanzania): Active tectonics and paleostress in the Ufipa plateau and Rukwa basin. *Journal of Structural Geology*, 37, 161–180. <https://doi.org/10.1016/j.jsg.2012.01.008>
- De Waele, B., & Mapani, B. (2002). Geology and correlation of the central Irumide belt. *Journal of African Earth Sciences*, 35(3), 385–397. [https://doi.org/10.1016/s0899-5362\(02\)00149-5](https://doi.org/10.1016/s0899-5362(02)00149-5)
- Diener, J. F. A., & Fagereng, A. (2014). The influence of melting and melt drainage on crustal rheology during orogenesis. *Journal of Geophysical Research: Solid Earth*, 119(8), 6193–6210. <https://doi.org/10.1002/2014jb011088>
- Diener, J. F. A., White, R. W., & Powell, R. (2008). Granulite facies metamorphism and subsolidus fluid-absent reworking, Strangways Range, Arunta Block, central Australia. *Journal of Metamorphic Geology*, 26(6), 603–622. <https://doi.org/10.1111/j.1525-1314.2008.00782.x>
- Dixey, F., Smith, W. C., & Bisset, C. B. (1937). *The Chilwa series of southern Nyasaland* (Bulletin No. 5). The Geological Survey of Nyasaland.
- Dolan, J. F., Bowman, D. D., & Sammis, C. G. (2007). Long-range and long-term fault interactions in Southern California. *Geology*, 35(9), 855–858. <https://doi.org/10.1130/g23789a.1>
- Druguet, E., Alsop, G. I., & Carreras, J. (2009). Coeval brittle and ductile structures associated with extreme deformation partitioning in a multilayer sequence. *Journal of Structural Geology*, 31(5), 498–511. <https://doi.org/10.1016/j.jsg.2009.03.004>

- Ebinger, C. J., Keir, D., Bastow, I. D., Whaler, K., Hammond, J. O., Ayele, A., et al. (2017). Crustal structure of active deformation zones in Africa: Implications for global crustal processes. *Tectonics*, *36*(12), 3298–3332. <https://doi.org/10.1002/2017TC004526>
- Ebinger, C. J., Oliva, S. J., Pham, T.-Q., Peterson, K., Chindandali, P., Illsley-Kemp, F., et al. (2019). Kinematics of active deformation in the Malawi Rift and Rungwe Volcanic Province, Africa. *Geochemistry, Geophysics, Geosystems*, *20*(8), 3928–3951. <https://doi.org/10.1029/2019gc008354>
- Ebinger, C. J., Rosendahl, B. R., & Reynolds, D. J. (1987). Tectonic model of the Malawi Rift, Africa. *Tectonophysics*, *141*(1–3), 215–235. [https://doi.org/10.1016/0040-1951\(87\)90187-9](https://doi.org/10.1016/0040-1951(87)90187-9)
- Engdahl, E. R., Di Giacomo, D., Sakarya, B., Gkarlaoui, C. G., Harris, J., & Storchak, D. A. (2020). ISC-EHB 1964–2016, an improved data set for studies of Earth structure and global seismicity. *Earth and Space Science*, *7*(1), e2019EA000897. <https://doi.org/10.1029/2019EA000897>
- Etheridge, M. A., Wall, V., Cox, S. F., & Vernon, R. (1984). High fluid pressures during regional metamorphism and deformation - Implications for mass transport and deformation mechanisms. *Journal of Geophysical Research*, *89*(B6), 4344–4358. <https://doi.org/10.1029/jb089ib06p04344>
- Fagereng, A. (2013). Fault segmentation, deep rift earthquakes and crustal rheology: Insights from the 2009 Karonga sequence and seismicity in the Rukwa–Malawi Rift zone. *Tectonophysics*, *601*, 216–225. <https://doi.org/10.1016/j.tecto.2013.05.012>
- Fagereng, A., & Beall, A. (2021). Is complex fault zone behaviour a reflection of rheological heterogeneity? *Philosophical Transactions of the Royal Society A*, *379*(2193), 20190421. <https://doi.org/10.1098/rsta.2019.0421>
- Fagereng, A., & Diener, J. F. A. (2011). San Andreas Fault tremor and retrograde metamorphism. *Geophysical Research Letters*, *38*(23), L23303. <https://doi.org/10.1029/2011GL049550>
- Fagereng, A., & Ikari, M. J. (2020). Low-temperature frictional characteristics of chlorite-epidote-amphibolite assemblages: Implications for strength and seismic style of retrograde fault zones. *Journal of Geophysical Research: Solid Earth*, *125*(4), e2020JB019487. <https://doi.org/10.1029/2020JB019487>
- Fagereng, A., & Sibson, R. H. (2010). Melange rheology and seismic style. *Geology*, *38*(8), 751–754. <https://doi.org/10.1130/G30868.1>
- Fritz, H., Abdelsalam, M., Ali, K. A., Bingen, B., Collins, A. S., Fowler, A. R., et al. (2013). Orogen styles in the East African Orogen: A review of the Neoproterozoic to Cambrian tectonic evolution. *Journal of African Earth Sciences*, *86*, 65–106. <https://doi.org/10.1016/j.jafrearsci.2013.06.004>
- Gaherty, J. B., Zheng, W., Shillington, D. J., Pritchard, M. E., Henderson, S. T., Chindandali, P. R. N., et al. (2019). Faulting processes during early-stage rifting: Seismic and geodetic analysis of the 2009–2010 Northern Malawi earthquake sequence. *Geophysical Journal International*, *217*(3), 1767–1782. <https://doi.org/10.1093/gji/ggz119>
- Gardonio, B., Jolivet, R., Calais, E., & Leclère, H. (2018). The April 2017  $M_w$  6.5 Botswana earthquake: An intraplate event triggered by deep fluids. *Geophysical Research Letters*, *45*(17), 8886–8896. <https://doi.org/10.1029/2018gl078297>
- Geological Survey of Malawi. (1966). *Geological map of Malawi, scale 1/1,000,000*. Geological Survey of Malawi.
- Goodwin, L. B., & Tikoff, B. (2002). Competency contrast, kinematics and the development of foliations and lineations in the crust. *Journal of Structural Geology*, *24*(6–7), 1065–1085. [https://doi.org/10.1016/s0191-8141\(01\)00092-x](https://doi.org/10.1016/s0191-8141(01)00092-x)
- Green, E. C. R., White, R. W., Diener, J. F. A., Powell, R., Holland, T. J. B., & Palin, R. M. (2016). Activity–composition relations for the calculation of partial melting equilibria in metabasic rocks. *Journal of Metamorphic Geology*, *34*(9), 845–869. <https://doi.org/10.1111/jmg.12211>
- Griggs, D. T., & Blacic, J. D. (1965). Anomalous weakness of synthetic crystals. *Science*, *147*(3655), 292–295. <https://doi.org/10.1126/science.147.3655.292>
- Haines, S., Lynch, E., Mulch, A., Valley, J. W., & van der Pluijm, B. (2016). Meteoric fluid infiltration in crustal-scale normal fault systems as indicated by  $\delta^{18}\text{O}$  and  $\delta^2\text{H}$  geochemistry and  $^{40}\text{Ar}/^{39}\text{Ar}$  dating of neofomed clays in brittle fault rocks. *Lithosphere*, *8*(6), 587–600. <https://doi.org/10.1130/L483.1>
- Handy, M. R. (1994). Flow laws for rocks containing two non-linear viscous phases: A phenomenological approach. *Journal of Structural Geology*, *16*(3), 287–301. [https://doi.org/10.1016/0191-8141\(94\)90035-3](https://doi.org/10.1016/0191-8141(94)90035-3)
- Handy, M. R., Wissing, S., & Streit, L. (1999). Frictional-viscous flow in mylonite with varied biminerallitic composition and its effect on lithospheric strength. *Tectonophysics*, *303*(1–4), 175–191. [https://doi.org/10.1016/s0040-1951\(98\)00251-0](https://doi.org/10.1016/s0040-1951(98)00251-0)
- Hellebrekers, N., Niemeijer, A. R., Fagereng, A., Manda, B., & Mvula, R. L. S. (2019). Lower crustal earthquakes in the East African Rift System: Insights from frictional properties of rock samples from the Malawi Rift. *Tectonophysics*, *767*, 228167. <https://doi.org/10.1016/j.tecto.2019.228167>
- Hodge, M., Biggs, J., Fagereng, A., Mdala, H., Wedmore, L. N. J., & Williams, J. N. (2020). Evidence from high-resolution topography for multiple earthquakes on high slip-to-length fault scarps: The Bilila-Mtakataka fault, Malawi. *Tectonics*, *39*(2), e2019TC005933. <https://doi.org/10.1029/2019TC005933>
- Hodge, M., Fagereng, A., Biggs, J., & Mdala, H. (2018). Controls on early-rift geometry: New perspectives from the Bilila-Mtakataka fault, Malawi. *Geophysical Research Letters*, *45*(9), 3896–3905. <https://doi.org/10.1029/2018gl077343>
- Hodgson, I., Illsley-Kemp, F., Gallacher, R. J., Keir, D., Ebinger, C. J., & Mtelega, K. (2017). Crustal structure at a young continental rift: A receiver function study from the Tanganyika Rift. *Tectonics*, *36*(12), 2806–2822. <https://doi.org/10.1002/2017TC004477>
- Holland, T., & Powell, R. (2011). An improved and extended internally consistent thermodynamic dataset for phases of petrological interest, involving a new equation of state for solids. *Journal of Metamorphic Geology*, *29*(3), 333–383. <https://doi.org/10.1111/j.1525-1314.2010.00923.x>
- Hopper, E., Gaherty, J. B., Shillington, D. J., Accardo, N. J., Nyblade, A. A., Holtzman, B. K., et al. (2020). Preferential localized thinning of lithospheric mantle in the melt-poor Malawi Rift. *Nature Geoscience*, *13*(8), 584–589. <https://doi.org/10.1038/s41561-020-0609-y>
- Imber, J., Holdsworth, R. E., Butler, C., & Lloyd, G. E. (1997). Fault-zone weakening processes along the reactivated Outer Hebrides Fault Zone, Scotland. *Journal of the Geological Society*, *154*(1), 105–109. <https://doi.org/10.1144/gsjgs.154.1.0105>
- Jackson, J. A., Austrheim, H., McKenzie, D., & Priestley, K. (2004). Metastability, mechanical strength, and the support of mountain belts. *Geology*, *32*(7), 625–628. <https://doi.org/10.1130/g20397.1>
- Jackson, J. A., & Blenkinsop, T. (1993). The Malawi Earthquake of March 10, 1989: Deep faulting within the East African Rift System. *Tectonics*, *12*(5), 1131–1139. <https://doi.org/10.1029/93TC01064>
- Jackson, J. A., & Blenkinsop, T. (1997). The Bilila-Mtakataka fault in Malawi: An active, 100-km long, normal fault segment in thick seismogenic crust. *Tectonics*, *16*(1), 137–150. <https://doi.org/10.1029/96tc02494>
- Jaeger, J., Cook, N. G. W., & Zimmerman, R. W. (2007). *Fundamentals of rock mechanics* (4th ed.). John Wiley.
- Jamveit, B., Ben-Zion, Y., Renard, F., & Austrheim, H. (2018). Earthquake-induced transformation of the lower crust. *Nature*, *556*(7702), 487–490. <https://doi.org/10.1038/s41586-018-0045-y>

- Jamtveit, B., Peltely-Ragan, A., Incel, S., Dunkel, K. G., Aupart, C., Austrheim, H., et al. (2019). The effects of earthquakes and fluids on the metamorphism of the lower continental crust. *Journal of Geophysical Research: Solid Earth*, *124*(8), 7725–7755. <https://doi.org/10.1029/2018jb016461>
- Janecke, S. U., & Evans, J. P. (1988). Feldspar-influenced rock rheologies. *Geology*, *16*(12), 1064–1067. [https://doi.org/10.1130/0091-7613\(1988\)016<1064:FIRR>2.3.CO;2](https://doi.org/10.1130/0091-7613(1988)016<1064:FIRR>2.3.CO;2)
- Jaupart, C., Mareschal, J.-C., & Iarotsky, L. (2016). Radiogenic heat production in the continental crust. *Lithos*, *262*, 398–427. <https://doi.org/10.1016/j.lithos.2016.07.017>
- Jones, D. J. R. (2020). *A summary of the East Africa Rift Temperature and Heat flow Model (EARTH)* (Open Report No. OR/20/006). British Geological Survey.
- Julià, J., Ammon, C. J., & Nyblade, A. A. (2005). Evidence for mafic lower crust in Tanzania, East Africa, from joint inversion of receiver functions and Rayleigh wave dispersion velocities. *Geophysical Journal International*, *162*(2), 555–569. <https://doi.org/10.1111/j.1365-246X.2005.02685.x>
- Kachingwe, M., Nyblade, A., & Julia, J. (2015). Crustal structure of Precambrian terranes in the southern African subcontinent with implications for secular variation in crustal genesis. *Geophysical Journal International*, *202*(1), 533–547. <https://doi.org/10.1093/gji/ggv136>
- Karamakar, S., & Schenk, V. (2016). Mesoproterozoic UHT metamorphism in the Southern Irumide Belt, Chipata, Zambia: Petrology and in situ monazite dating. *Precambrian Research*, *275*, 332–356. <https://doi.org/10.1016/j.precamres.2016.01.018>
- Kendall, J.-M., & Lithgow-Bertelloni, C. (2016). Why is Africa rifting? *Geological Society, London, Special Publications*, *420*(1), 11–30. <https://doi.org/10.1144/SP420.1>
- Kolawole, F., Atekwana, E. A., Laó-Dávila, D. A., Abdelsalam, M., Chindandali, P., Salima, J., & Kalindekafe, L. (2018). Active deformation of Malawi Rift's north basin Hinge zone modulated by reactivation of preexisting Precambrian Shear zone fabric. *Tectonics*, *37*(3), 683–704. <https://doi.org/10.1002/2017tc004628>
- Kröner, A., Willner, A., Hegner, E., Jaekel, P., & Nemchin, A. (2001). Single zircon ages, PT evolution and Nd isotopic systematics of high-grade gneisses in southern Malawi and their bearing on the evolution of the Mozambique belt in southeastern Africa. *Precambrian Research*, *109*(3–4), 257–291. [https://doi.org/10.1016/S0301-9268\(01\)00150-4](https://doi.org/10.1016/S0301-9268(01)00150-4)
- Laó Dávila, D. A., Al-Salmi, H. S., Abdelsalam, M. G., Atekwana, E. A. (2015). Hierarchical segmentation of the Malawi Rift: The influence of inherited lithospheric heterogeneity and kinematics in the evolution of continental rifts. *Tectonics*, *34*(12), 2399–2417. <https://doi.org/10.1002/2015TC003953>
- Lavayssière, A., Drooff, C., Ebinger, C., Gallacher, R., Illsley-Kemp, F., Oliva, S. J., & Keir, D. (2019). Depth extent and kinematics of faulting in the southern Tanganyika Rift, Africa. *Tectonics*, *38*(3), 842–862. <https://doi.org/10.1029/2018TC005379>
- Lee, H., Muirhead, J. D., Fischer, T. P., Ebinger, C. J., Kattenhorn, S. A., Sharp, Z. D., & Kianji, G. (2016). Massive and prolonged deep carbon emissions associated with continental rifting. *Nature Geoscience*, *9*(2), 145–149. <https://doi.org/10.1038/ngeo2622>
- Lindenfeld, M., Rumpker, G., Link, K., Koehn, D., & Batte, A. (2012). Fluid-triggered earthquake swarms in the Rwenzori region, East African Rift - Evidence for rift initiation. *Tectonophysics*, *566–567*, 95–104. <https://doi.org/10.1016/j.tecto.2012.07.010>
- Lu, L. X., & Jiang, D. (2019). Quartz flow law revisited: The significance of pressure dependence of the activation enthalpy. *Journal of Geophysical Research: Solid Earth*, *124*(1), 241–256. <https://doi.org/10.1029/2018jb016226>
- Maggi, A., Jackson, J. A., McKenzie, D., & Priestly, K. (2000). Earthquake focal depths, effective elastic thickness, and the strength of continental lithosphere. *Geology*, *28*(6), 495–498. [https://doi.org/10.1130/0091-7613\(2000\)28<495:efdeet>2.0.co;2](https://doi.org/10.1130/0091-7613(2000)28<495:efdeet>2.0.co;2)
- Manda, B. W. C., Cawood, P. A., Spencer, C. J., Prave, T., Robinson, R., & Roberts, N. M. W. (2019). Evolution of the Mozambique Belt in Malawi constrained by granitoid U-Pb, Sm-Nd and Lu-Hf isotopic data. *Gondwana Research*, *68*, 93–107. <https://doi.org/10.1016/j.gr.2018.11.004>
- Mareschal, J.-C., & Jaupart, C. (2013). Radiogenic heat production, thermal regime and evolution of continental crust. *Tectonophysics*, *609*, 524–534. <https://doi.org/10.1016/j.tecto.2012.12.001>
- McKenzie, D., & Fairhead, D. (1997). Estimates of the effective elastic thickness of the continental lithosphere from Bouguer and free air gravity anomalies. *Journal of Geophysical Research*, *102*(B12), 27523–27552. <https://doi.org/10.1029/97jb02481>
- McKenzie, D., Jackson, J. A., & Priestly, K. (2005). Thermal structure of oceanic and continental lithosphere. *Earth and Planetary Science Letters*, *233*(3–4), 337–349. <https://doi.org/10.1016/j.epsl.2005.02.005>
- McMillan, M. F., Boone, S. C., Kohn, B. P., Gleadow, A. J., & Chindandali, P. R. (2022). Development of the Nyika Plateau, Malawi: A long lived paleo-surface or a contemporary feature of the East African Rift? *Geochemistry, Geophysics, Geosystems*, *23*(8), e2022GC01390. <https://doi.org/10.1029/2022GC010390>
- Menegon, L., & Fagereng, A. (2021). Tectonic pressure gradients during viscous creep drive fluid flow and brittle failure at the base of the seismogenic zone. *Geology*, *49*(10), 1255–1259. <https://doi.org/10.1130/g49012.1>
- Mildon, Z. K., Roberts, G. P., Faure Walker, J. P., Beck, J., Papanikolaou, I., Michetti, A. M., et al. (2022). Surface faulting earthquake clustering controlled by fault and shear-zone interactions. *Nature Communications*, *13*(1), 7126. <https://doi.org/10.1038/s41467-022-34821-5>
- Montési, L. G. (2013). Fabric development as the key for forming ductile shear zones and enabling plate tectonics. *Journal of Structural Geology*, *50*, 254–266. <https://doi.org/10.1016/j.jsg.2012.12.011>
- Mortimer, E., Kirstein, L. A., Stuart, F. M., & Strecker, M. R. (2016). Spatio-temporal trends in normal-fault segmentation recorded by low-temperature thermochronology: Livingston fault scarp, Malawi Rift, East African Rift System. *Earth and Planetary Science Letters*, *455*, 62–72. <https://doi.org/10.1016/j.epsl.2016.08.040>
- Muirhead, J. D., Kattenhorn, S. A., Lee, H., Mana, S., Turrin, B. D., Fischer, T. P., et al. (2016). Evolution of upper crustal faulting assisted by magmatic volatile release during early-stage continental rift development in the East African Rift. *Geosphere*, *12*(6), 1670–1700. <https://doi.org/10.1130/GES01375.1>
- Njinju, E. A., Atekwana, E. A., Stamps, D. S., Abdelsalam, M. G., Atekwana, E. A., Mickus, K. L., et al. (2019a). Lithospheric structure of the Malawi Rift: Implications for magma-poor rifting processes. *Tectonics*, *38*(11), 3835–3853. <https://doi.org/10.1029/2019tc005549>
- Njinju, E. A., Kolawole, F., Atekwana, E. A., Stamps, D. S., Atekwana, E. A., Abdelsalam, M. G., & Mickus, K. L. (2019b). Terrestrial heat flow in the Malawi Rifted Zone, East Africa: Implications for tectono-thermal inheritance in continental rift basins. *Journal of Volcanology and Geothermal Research*, *387*, 106656. <https://doi.org/10.1016/j.jvolgeores.2019.07.023>
- Norris, R. J., & Henley, R. W. (1976). Dewatering of a metamorphic pile. *Geology*, *4*(6), 333–336. [https://doi.org/10.1130/0091-7613\(1976\)4<333:doamp>2.0.co;2](https://doi.org/10.1130/0091-7613(1976)4<333:doamp>2.0.co;2)
- Nyalugue, V. N., Abdelsalam, M. G., Atekwana, E. A., Katumwehe, A., Mickus, K. L., Salima, J., et al. (2019). Lithospheric structure beneath the Cretaceous Chilwa Alkaline Province (CAP) in southern Malawi and northeastern Mozambique. *Journal of Geophysical Research: Solid Earth*, *124*(11), 12224–12240. <https://doi.org/10.1029/2019JB018430>

- Nyblade, A. A., & Langston, C. A. (1995). East African earthquakes below 20 km depth and their implications for crustal structure. *Geophysical Journal International*, *121*(1), 49–62. <https://doi.org/10.1111/j.1365-246x.1995.tb03510.x>
- Ojo, O. O., Ohenhen, L. O., Kolawole, F., Johnson, S. G., Chindandali, P. R., Atekwana, E. A., & Laó-Dávila, D. A. (2022). Under-displaced normal faults: Strain accommodation along an early-stage rift-bounding fault in the southern Malawi Rift. *Frontiers in Earth Science*, *10*, 846389. <https://doi.org/10.3389/feart.2022.846389>
- Pennacchioni, G., & Mancktelow, N. S. (2007). Nucleation and initial growth of a shear zone network within compositionally and structurally heterogeneous granitoids under amphibolite facies conditions. *Journal of Structural Geology*, *29*(11), 1757–1780. <https://doi.org/10.1016/j.jsg.2007.06.002>
- Petitjean, S., Rabinowicz, M., Grégoire, M., & Chevrot, S. (2006). Differences between Archean and Proterozoic lithospheres: Assessment of the possible major role of thermal conductivity. *Geochemistry, Geophysics, Geosystems*, *7*(3), 1–26. <https://doi.org/10.1029/2005gc001053>
- Powell, R., & Holland, T. (1988). An internally consistent dataset with uncertainties and correlations: 3. Applications to geobarometry, worked examples and a computer program. *Journal of Metamorphic Geology*, *6*(2), 173–204. <https://doi.org/10.1111/j.1525-1314.1988.tb00415.x>
- Rennie, S. F., Fagereng, A., & Diener, J. F. A. (2013). Strain distribution within a km-scale, mid-crustal shear zone: The Kuckaus Mylonite Zone, Namibia. *Journal of Structural Geology*, *56*, 57–69. <https://doi.org/10.1016/j.jsg.2013.09.001>
- Ring, U. (1995). Tectonic and lithological constraints on the evolution of the Karoo graben of northern Malawi (East Africa). *Geologische Rundschau*, *84*(3), 607–625. <https://doi.org/10.1007/BF00284524>
- Ring, U., Kröner, A., & Toulkeridis, T. (1997). Palaeoproterozoic granulite-facies metamorphism and granitoid intrusions in the Ubendian–Usagaran Orogen of northern Malawi, east-central Africa. *Precambrian Research*, *85*(1–2), 27–51. [https://doi.org/10.1016/s0301-9268\(97\)00028-4](https://doi.org/10.1016/s0301-9268(97)00028-4)
- Roecker, S., Ebinger, C. J., Tiberi, C., Mulibo, G., Ferdinand-Wambura, R., Mtelega, K., et al. (2017). Subsurface images of the Eastern Rift, Africa, from the joint inversion of body waves, surface waves and gravity: Investigating the role of fluids in early-stage continental rifting. *Geophysical Journal International*, *210*(2), 931–950. <https://doi.org/10.1093/gji/ggx220>
- Rosenberg, C. L., & Handy, M. R. (2005). Experimental deformation of partially melted granite revisited: Implications for continental crust. *Journal of Metamorphic Geology*, *23*(1), 19–28. <https://doi.org/10.1111/j.1525-1314.2005.00555.x>
- Ruh, J. B., Tokle, L., & Behr, W. M. (2022). Grain-size-evolution controls on lithospheric weakening during continental rifting. *Nature Geoscience*, *15*(7), 585–590. <https://doi.org/10.1038/s41561-022-00964-9>
- Rybacki, E., & Dresen, G. (2000). Dislocation and diffusion creep of synthetic anorthite aggregates. *Journal of Geophysical Research*, *105*(B11), 26017–26036. <https://doi.org/10.1029/2000jb900223>
- Rybacki, E., & Dresen, G. (2004). Deformation mechanism maps for feldspar rocks. *Tectonophysics*, *382*(3), 173–187. <https://doi.org/10.1016/j.tecto.2004.01.006>
- Samsu, A., Micklethwaite, S., Williams, J. N., Fagereng, A., & Cruden, A. R. (2023). Structural inheritance in amagmatic rift basins: Manifestations and mechanisms for how pre-existing structures influence rift-related faults. *Earth-Science Reviews*, *246*, 104568. <https://doi.org/10.1016/j.earscirev.2023.104568>
- Shinevar, W. J., Behn, M. D., & Hirth, G. (2015). Compositional dependence of lower crustal viscosity. *Geophysical Research Letters*, *42*(20), 8333–8340. <https://doi.org/10.1002/2015gl065459>
- Shudofsky, G. N., Cloething, S., Stein, S., & Wortel, R. (1987). Unusually deep earthquakes in East Africa: Constraints on the thermo-mechanical structure of a continental rift system. *Geophysical Research Letters*, *14*(7), 741–744. <https://doi.org/10.1029/g1014i007p00741>
- Sibson, R. H. (1980). Transient discontinuities in ductile shear zones. *Journal of Structural Geology*, *2*(1–2), 165–171. [https://doi.org/10.1016/0191-8141\(80\)90047-4](https://doi.org/10.1016/0191-8141(80)90047-4)
- Sibson, R. H. (2017). The edge of failure: Critical stress overpressure states in different tectonic regimes. *Geological Society, London, Special Publications*, *458*(1), 131–141. <https://doi.org/10.1144/SP458.5>
- Sloan, R. A., Jackson, J. A., McKenzie, D., & Priestly, K. (2011). Earthquake depth distributions in central Asia, and their relations with lithospheric thickness, shortening and extension. *Geophysical Journal International*, *185*, 1–29. <https://doi.org/10.1111/j.1365-246x.2010.04882.x>
- Stamps, D. S., Flesch, L. M., Calais, E., & Ghosh, A. (2014). Current kinematics and dynamics of Africa and the East African Rift System. *Journal of Geophysical Research: Solid Earth*, *119*(6), 5161–5186. <https://doi.org/10.1002/2013JB010717>
- Stenvall, C., Fagereng, A., Diener, J. F. A., Harris, C., & Janney, P. (2020). Sources and effects of fluids in continental retrograde shear zones: Insights from the Kuckaus Mylonite Zone, Namibia. *Geofluids*, *2020*, 1–21. <https://doi.org/10.1155/2020/3023268>
- Stevens, V., Sloan, R., Chindandali, P., Wedmore, L. N., Salomon, G., & Muir, R. (2021). The entire crust can be seismogenic: Evidence from southern Malawi. *Tectonics*, *40*(6), e2020TC006654. <https://doi.org/10.1029/2020tc006654>
- Sun, M., Gao, S. S., Liu, K. H., Mickus, K., Fu, X., & Yu, Y. (2021). Receiver function investigation of crustal structure in the Malawi and Luangwa rift zones and adjacent areas. *Gondwana Research*, *89*, 168–176. <https://doi.org/10.1016/j.gr.2020.08.015>
- Tenczer, V., Powell, R., & Stüwe, K. (2006). Evolution of H<sub>2</sub>O content in a polymetamorphic terrane: The Plattengneiss Shear Zone (Koralpe, Austria). *Journal of Metamorphic Geology*, *24*(4), 281–295. <https://doi.org/10.1111/j.1525-1314.2006.00637.x>
- Thomas, R. J., Fullgraf, T., Macey, P. H., Boger, S. D., Hölttä, P., Lach, P., et al. (2022). The Mesoproterozoic Nampula subdomain in southern Malawi: Completing the story from Mozambique. *Journal of African Earth Sciences*, *196*, 104667. <https://doi.org/10.1016/j.jafrearsci.2022.104667>
- Tikoff, B., & Teyssier, C. (1994). Strain modeling of displacement-field partitioning in transpressional orogens. *Journal of Structural Geology*, *16*(11), 1575–1588. [https://doi.org/10.1016/0191-8141\(94\)90034-5](https://doi.org/10.1016/0191-8141(94)90034-5)
- Tsunogae, T., Uthup, S., Nyirongo, M. W., Takahashi, K., Rahman, M. S., Liu, Q., et al. (2021). Neoproterozoic crustal growth in southern Malawi: New insights from petrology, geochemistry, and U–Pb zircon geochronology, and implications for the Kalahari Craton–Congo Craton amalgamation. *Precambrian Research*, *352*, 106007. <https://doi.org/10.1016/j.precamres.2020.106007>
- Vail, J. (1989). Ring complexes and related rocks in Africa. *Journal of African Earth Sciences*, *8*(1), 19–40. [https://doi.org/10.1016/s0899-5362\(89\)80006-5](https://doi.org/10.1016/s0899-5362(89)80006-5)
- Versfelt, J., & Rosendahl, B. R. (1989). Relationships between pre-rift structure and rift architecture in Lakes Tanganyika and Malawi, East Africa. *Nature*, *337*(6205), 354–357. <https://doi.org/10.1038/337354a0>
- Von Herzen, R. P., & Vacquier, V. (1967). Terrestrial heat flow in Lake Malawi, Africa. *Journal of Geophysical Research*, *72*(16), 4221–4226. <https://doi.org/10.1029/jz072i016p04221>
- Wang, T., Feng, J., Liu, K. H., & Gao, S. S. (2019). Crustal structure beneath the Malawi and Luangwa Rift Zones and adjacent areas from ambient noise tomography. *Gondwana Research*, *67*, 187–198. <https://doi.org/10.1016/j.gr.2018.10.018>

- Wedmore, L. N. J., Biggs, J., Floyd, M., Fagereng, Å., Mdala, H., Chindandali, P., et al. (2021). Geodetic constraints on cratonic microplates and broad strain during rifting of thick Southern African lithosphere. *Geophysical Research Letters*, *48*(17), e2021GL093785. <https://doi.org/10.1029/2021gl093785>
- Wedmore, L. N. J., Williams, J. N., Biggs, J., Fagereng, A., Mphepo, F., Dulanya, Z., et al. (2020). Structural inheritance and border fault reactivation during active early-stage rifting along the Thyolo fault, Malawi. *Journal of Structural Geology*, *139*, 104097. <https://doi.org/10.1016/j.jsg.2020.104097>
- Weinstein, A., Oliva, S. J., Ebinger, C. J., Roecker, S., Tiberi, C., Aman, M., et al. (2017). Fault-magma interactions during early continental rifting: Seismicity of the Magadi-Natron-Manyara basins, Africa. *Geochemistry, Geophysics, Geosystems*, *18*(10), 3662–3686. <https://doi.org/10.1002/2017GC007027>
- Wheeler, W. H., & Karson, J. A. (1989). Structure and kinematics of the Livingston Mountains border fault zone, Nyasa (Malawi) Rift, southwestern Tanzania. *Journal of African Earth Sciences*, *8*(2–4), 393–413. [https://doi.org/10.1016/s0899-5362\(89\)80034-x](https://doi.org/10.1016/s0899-5362(89)80034-x)
- Wheeler, W. H., & Rosendahl, B. R. (1994). Geometry of the Livingston Mountains Border Fault, Nyasa (Malawi) Rift, East Africa. *Tectonics*, *13*(2), 303–312. <https://doi.org/10.1029/93TC02314>
- White, R. W., & Powell, R. (2002). Melt loss and the preservation of granulite facies mineral assemblages. *Journal of Metamorphic Geology*, *20*(7), 621–632. [https://doi.org/10.1046/j.1525-1314.2002.00206\\_20\\_7.x](https://doi.org/10.1046/j.1525-1314.2002.00206_20_7.x)
- White, R. W., Powell, R., & Halpin, J. A. (2004). Spatially-focussed melt formation in aluminous metapelites from Broken Hill, Australia. *Journal of Metamorphic Geology*, *22*(9), 825–845. <https://doi.org/10.1111/j.1525-1314.2004.00553.x>
- White, R. W., Powell, R., Holland, T. J. B., Johnson, T. E., & Green, E. C. R. (2014). New mineral activity–composition relations for thermodynamic calculations in metapelitic systems. *Journal of Metamorphic Geology*, *32*(3), 261–286. <https://doi.org/10.1111/jmg.12071>
- Williams, J. N., Fagereng, A., Wedmore, L. N. J., Biggs, J., Mdala, H., Mphepo, F., & Hodge, M. (2022a). Low dissipation of earthquake energy where a fault follows pre-existing weaknesses: Field and microstructural observations of Malawi's Bilila-Mtakataka fault. *Geophysical Research Letters*, *49*(8), e2021GL095286. <https://doi.org/10.1029/2021GL095286>
- Williams, J. N., Fagereng, A., Wedmore, L. N. J., Biggs, J., Mphepo, F., Dulanya, Z., et al. (2019). How do variably striking faults reactivate during rifting? Insights from southern Malawi. *Geochemistry, Geophysics, Geosystems*, *20*(7), 3588–3607. <https://doi.org/10.1029/2019gc008219>
- Williams, J. N., Wedmore, L. N. J., Fagereng, A., Werner, M. J., Mdala, H., Shillington, D. J., et al. (2022b). Geologic and geodetic constraints on the magnitude and frequency of earthquakes along Malawi's active faults: The Malawi Seismogenic Source Model (MSSM). *Natural Hazards and Earth System Sciences*, *22*(11), 3607–3639. <https://doi.org/10.5194/nhess-22-3607-2022>
- Williams, J. N., Wedmore, L. N. J., Scholz, C. A., Kolawole, F., Wright, L. J. M., Shillington, D. J., et al. (2022c). The Malawi Active Fault Database: An onshore-offshore database for regional assessment of seismic hazard and tectonic evolution. *Geochemistry, Geophysics, Geosystems*, *23*(5), e2022GC010425. <https://doi.org/10.1029/2022gc010425>
- Williams, J. N., Werner, M. J., Goda, K., Wedmore, L. N. J., De Risi, R., Biggs, J., et al. (2023). Fault-based probabilistic seismic hazard analysis in regions with low strain rates and a thick seismogenic layer: A case study from Malawi. *Geophysical Journal International*, *233*(3), 2172–2207. <https://doi.org/10.1093/gji/ggad060>
- Wintsch, R. P., Christoffersen, R., & Kronenberg, A. K. (1995). Fluid-rock reaction weakening of fault zones. *Journal of Geophysical Research*, *100*(B7), 13021–13032. <https://doi.org/10.1029/94jb02622>
- Yardley, B. W. D. (1983). Quartz veins and devolatilization during metamorphism. *Journal of the Geological Society*, *140*(4), 657–663. <https://doi.org/10.1144/gsjgs.140.4.0657>
- Yardley, B. W. D. (1986). Fluid migration and veining in the Connemara schists, Ireland. In J. Walther & B. Wood (Eds.), *Fluid-rock interactions during metamorphism* (pp. 109–131). Springer-Verlag.
- Yardley, B. W. D. (2009). The role of water in the evolution of the continental crust. *Journal of the Geological Society*, *166*(4), 585–600. <https://doi.org/10.1144/0016-76492008-101>